Symposium F.1
Chalcogenide Semiconductor Research and Applications
Tutorial

Chalcogenide electronic materials research: Computation, synthesis, characterization

First principles calculations of electronic structure, defects, disorder

Stephan Lany, National Renewable Energy Laboratory, Golden, CO

Thin film growth

Rafael Jaramillo, Massachusetts Institute of Technology, Cambridge, MA

High-throughput computation and thermoelectrics

Prashun Gorai, Colorado School of Mines and NREL, Golden, CO

Thin film characterization

Rafael Jaramillo

NREL
NATIONAL RENEWABLE ENERGY LABORATORY

Massachusetts Institute of Technology

MINES

NREL
NATIONAL RENEWABLE ENERGY LABORATORY

Tutorial

First principles calculations: Electronic structure, defects, disorder

Stephan Lany

National Renewable Energy Laboratory, Golden, CO

What do we want to predict by theory?

Properties of semiconductors

- **Structure (total-energy)**
  - Inter-atomic potentials (Lennard-Jones, Morse, VFF)
  - Electrostatic interactions
  - Quantum-mechanical (DFT)
- **Thermodynamic stability (total-energy)**
  - Quantum-mechanical (DFT)
- **Defects and doping (total-energy)**
  - Cavity model for vacancies
  - Model potentials (e.g., Morse)
  - Quantum-mechanical (DFT)
- **Band-structure (quasi-particle energies)**
  - Empirical (tight-binding, k·p, EPM, NLEP)
  - Quantum-mechanical (Hartree-Fock $\rightarrow$ CI, CC, MCSCF)
  - Quantum-mechanical (DFT $\rightarrow$ GW)

Working horse of electronic structure theory: *Local Density Approximation (LDA)*

Schrödinger's equation:

$$\hat{H}\psi = E\psi$$

General Quantum mechanics:

$$[\hat{T} + \hat{V}]\psi(\mathbf{r}_1,...,\mathbf{r}_N) = E\psi(\mathbf{r}_1,...,\mathbf{r}_N)$$

Density Functional Theory:

$$[\hat{T}_0 + \sum\nolimits_Z V_Z + \sum\nolimits_e V_e + V_{\mathrm{XC}}]\psi_i(\mathbf{r}) = \varepsilon_i\psi_i(\mathbf{r})$$

$$E_{\mathrm{DFT}} = T_0 + E_{ii} + E_{ei} + E_{ee} + E_{\mathrm{XC}}$$

$$E_{\mathrm{XC}} = \int n(\mathbf{r})\varepsilon_{\mathrm{XC}}[n,|\nabla n|]d\mathbf{r} \qquad V_{\mathrm{XC}}(\mathbf{r}) = \frac{\delta E_{\mathrm{XC}}(n)}{\delta n(\mathbf{r})}$$

ΣV_e includes self-interaction

V_{XC} corrects for SI, many-particle effects

Hohenberg-Kohn 1964, applications ~70s, Perdew–Zunger LDA 1981

- High accuracy for electronic density and total-energies
- Usually not sufficiently accurate for single-particle energies

Electronic structure and optical properties

Empirical approaches

- Empirical approaches for band structure calculation
  Tight-binding (LCAO), ***k·p***, **empirical pseudopotentials**

$$\left(-\tfrac{1}{2}\nabla^2 + \sum_{\alpha,n} v_\alpha(|\mathbf{r}-\mathbf{R}_{\alpha,n}|)\right)\psi_{i,\mathbf{k}}(\mathbf{r}) = e_{i,\mathbf{k}}\psi_{i,\mathbf{k}}(\mathbf{r})$$

(1) Fit parameters to reference data
(experiment, accurate theory)

(2) Assuming transferability,
apply to more complex cases
Full BZ, alloys, nanostructures, ...

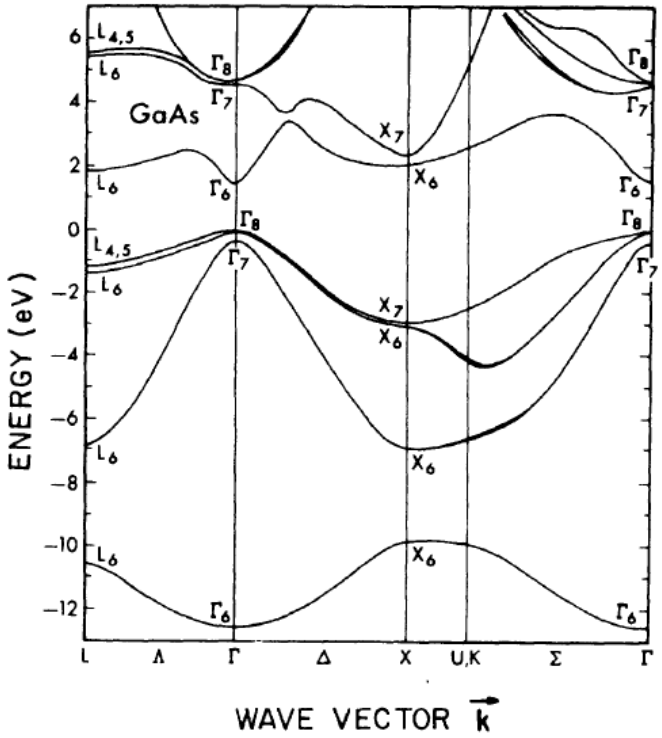

Energy-band interpolation scheme based on a pseudopotential
J.C. Phillips, Phys. Rev. **112**, 685 (1958)

Nonlocal pseudopotential calculations for the electronic structure of eleven diamond and zinc-blende semiconductors
J.R. Chelikowsky, M.L. Cohen, Phys. Rev. B **14**, 556 (1976)

Properties for energy materials: Band structure calculation

Importance of electronic-structure

- Band-gaps, band-structure, optical properties (α, ε), transport: effective masses
- Energy materials: Photovoltaics, solar fuels, thermoelectrics, electronic materials, battery materials

Band-structures and band gaps with DFT starting point

- Starting from DFT, calculate electron self energy Σ, get quasiparticle energy correction to DFT

$$e_n^{GW} = e_n^{\mathrm{DFT}} + \mathrm{Re}\left\langle \psi_n^{\mathrm{DFT}} \middle| \Sigma(e_n^{GW}) - V_{\mathrm{xc}}^{\mathrm{DFT}} \middle| \psi_n^{\mathrm{DFT}} \right\rangle$$

GW approximation for self energy Σ

G: Green's function, W: screened Coulomb interaction

- GW uses the ***screened*** Coulomb potential (*cf.* "screened exchange")

$$\Sigma(\mathbf{r},\mathbf{r}',\omega) = \frac{i}{4\pi}\int_{-\infty}^{\infty} e^{i\omega'\delta} G(\mathbf{r},\mathbf{r}',\omega+\omega') W(\mathbf{r},\mathbf{r}',\omega') d\omega'$$

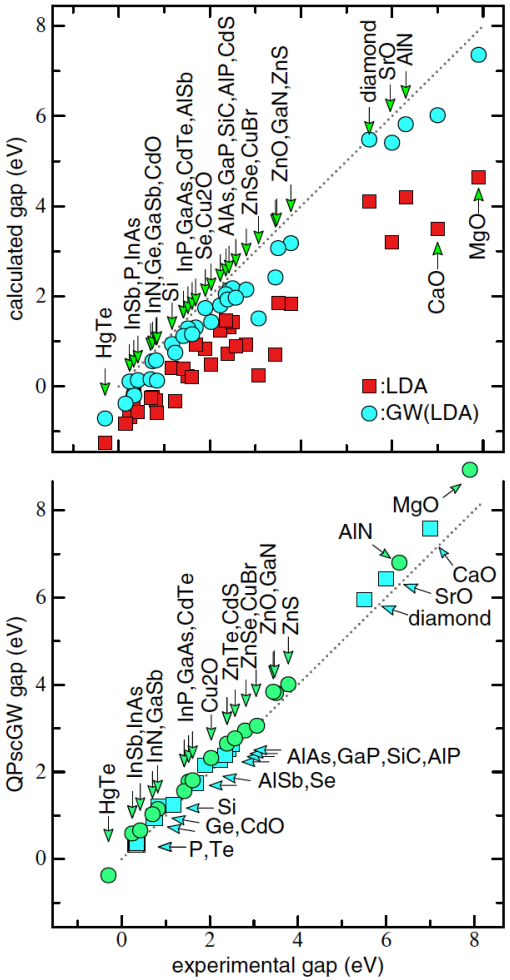

For main group compounds, GW calculations give band gaps in very good agreement with experiment

M. van Schilfgaarde *et al.*, PRL **96**, 226402 (2006)

GW calculation of band-structure and optical properties

- Many-body perturbation theory in GW approximation implemented in numerous codes (VASP, BerkeleyGW, Questaal, Yambo)
- More demanding than DFT calculations:
  - CPU and memory requirements
  - Convergence, self-consistency, vertex-corrections
  - 3d transition metals
- Optical properties from dielectric function $\varepsilon(\omega) + i\varepsilon_2(\omega)$
  - independent particle approximation
  - Bethe-Salpeter equation (excitonic effects)

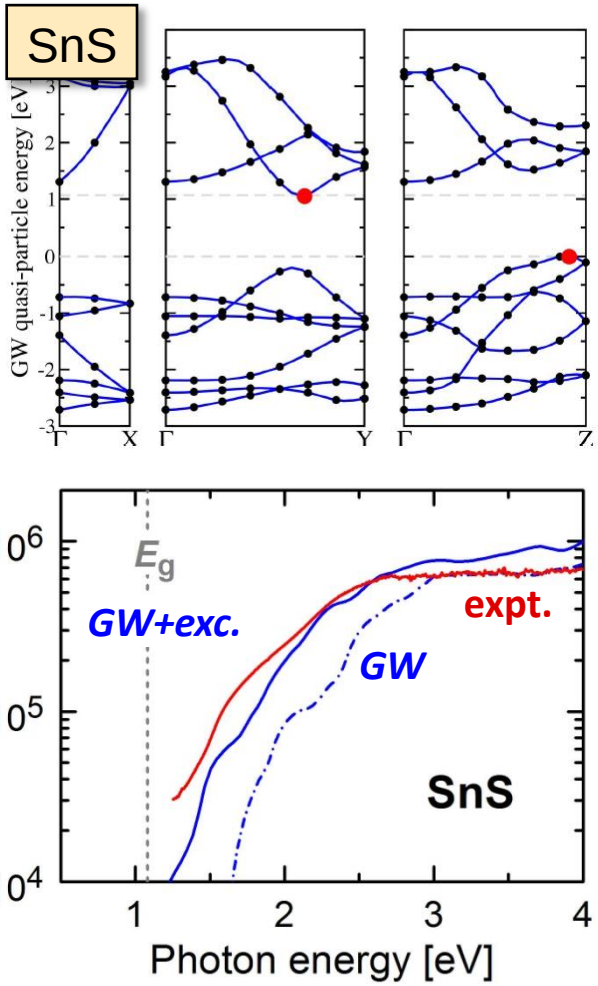

J. Vidal *et al.*, Appl. Phys. Lett. **100**, 032104 (2012)

Implementation and performance of the frequency-dependent GW method within the PAW framework, M. Shishkin, G. Kresse, Phys. Rev. B **74**, 035101 (2006)

Dielectric properties and excitons for extended systems from hybrid functionals, J. Paier, M. Marsman, and G. Kresse, Phys. Rev. B **78**, 121201(R) (2008)

Transition metal compounds: Band vs Mott insulator

Band insulator

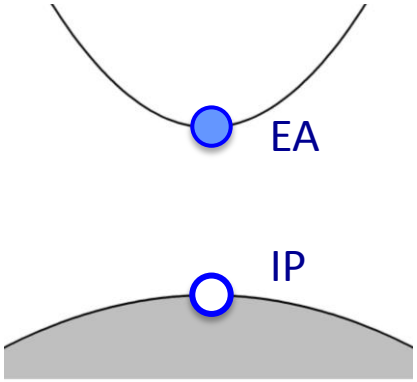

Mott insulator

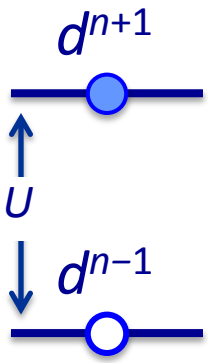

Charge transfer insulator

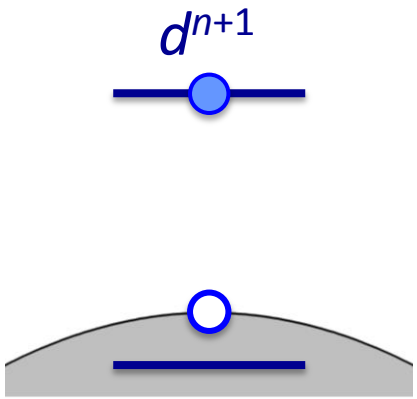

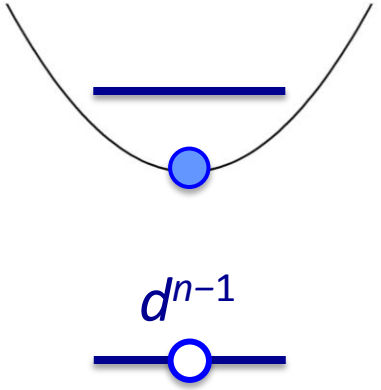

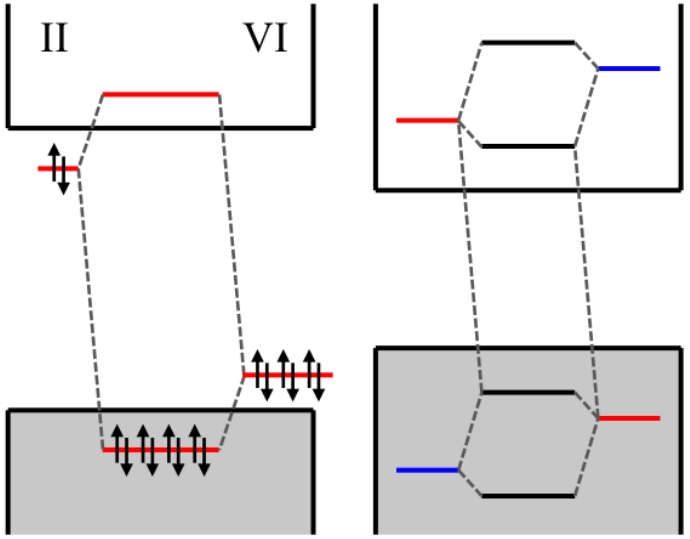

- Dispersion of *d* states
- Hybridization of *d* and *sp*
- *d* and *sp* states on same footing
- Band gap, effective masses
- Doping, defects, compensation
- Band vs small polaron transport

Band gap prediction: GW scheme for transition metal oxides

- GW method is computationally expensive and converges slowly
- Transition metal oxides are even more challenging due to localized d-electrons
- Standard GW(RPA) scheme that works well for main group compounds overestimates gaps for TM oxides (TiO_2, ..., Cu_2O)
- Approach: GW with additional potential term for *d*-orbital energies (GW+V_d)

$$\hat{V} = \sum_{i,j} \left| p_i \right\rangle \left\langle \phi_i^{\mathrm{AE}} \left| V_{\mathrm{d}} \right| \phi_j^{\mathrm{AE}} \right\rangle \left\langle p_j \right|$$

- One empirical parameter per TM atom, but applicable for (semi-) high-throughput band gap prediction for 100s of materials

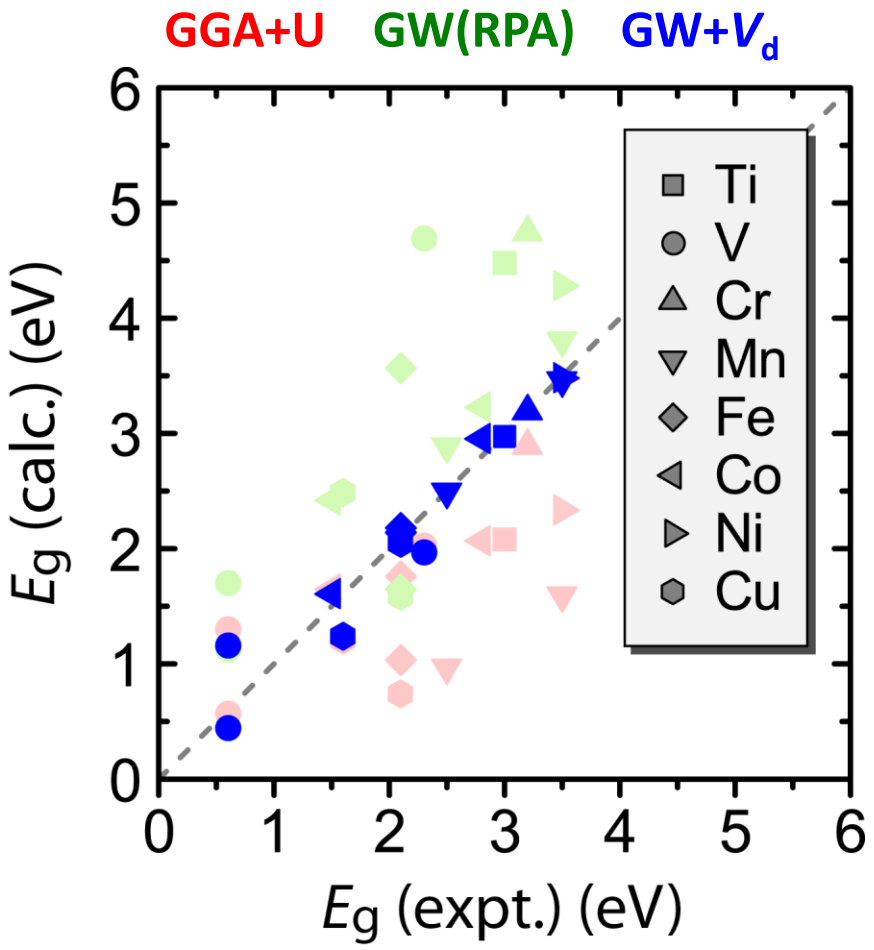

SL, Phys. Rev. B **87**, 085112 (2013)

Example: GW+V_d for copper oxides

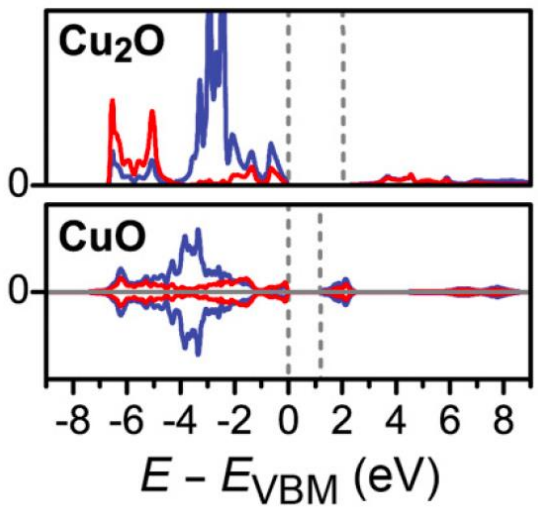

- Cu-*d*: V_d= −2.4 eV; good band gaps for both **Cu_2O** (direct-forbidden 2.04 eV) and **CuO** (indirect 1.24 eV) note: expt. E_g = 1.6 eV is direct
- Correct Γ_1 - Γ_{12} band ordering in Cu_2O (wrong in GW-RPA)
- Absorption coefficient in near-quantitative agreement with experiment
- Band-edge shifts useful for defect calculations, band-offsets, IP/EA

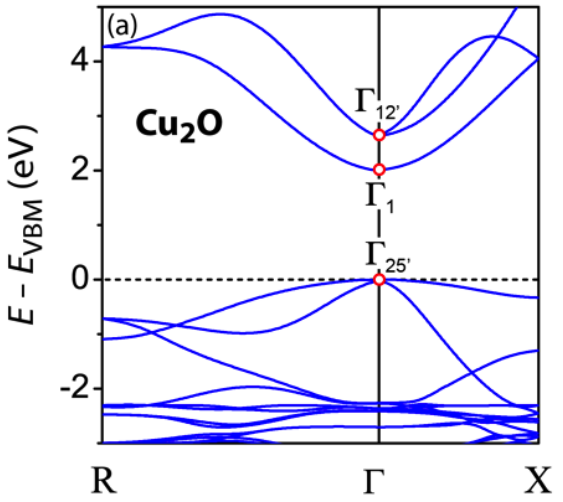

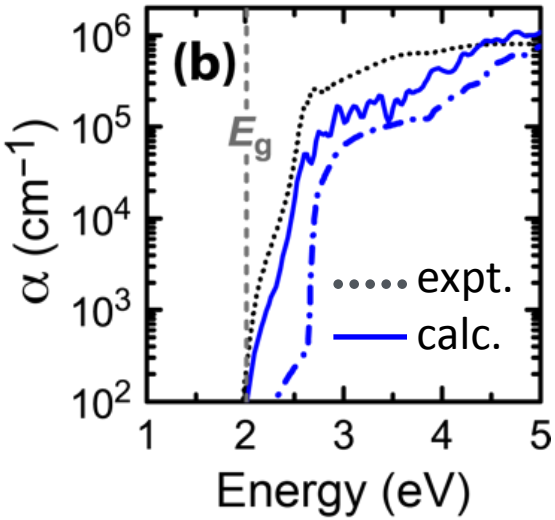

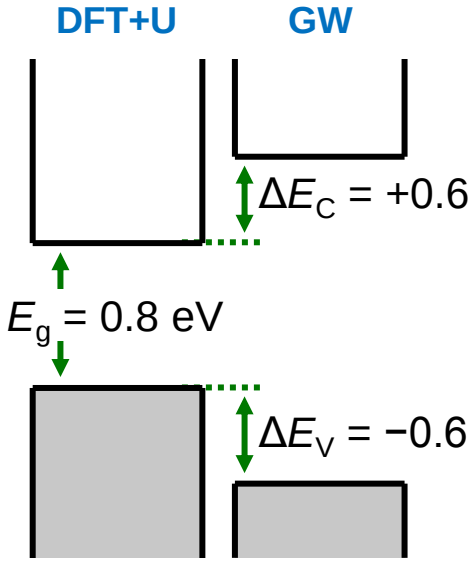

Coulomb gap in CoO

- Mott insulators often defined by breakdown of band theory
- CoO has large gap between occupied and unoccupied t_2 spin-dn crystal field levels (Coulomb gap)
- Quasi-closed shell configuration: crystal field splitting (t_2, e) spin exchange splitting only occ. or empty spin/cf levels
- Tetrahedral Co^{+II} QCS; Co_3O_4, ZnO:Co zinc-blende CoO lowest E in GGA+U Co-s like CBM, $m_e^* = 0.5\ m_0$ (DOS-effective mass)

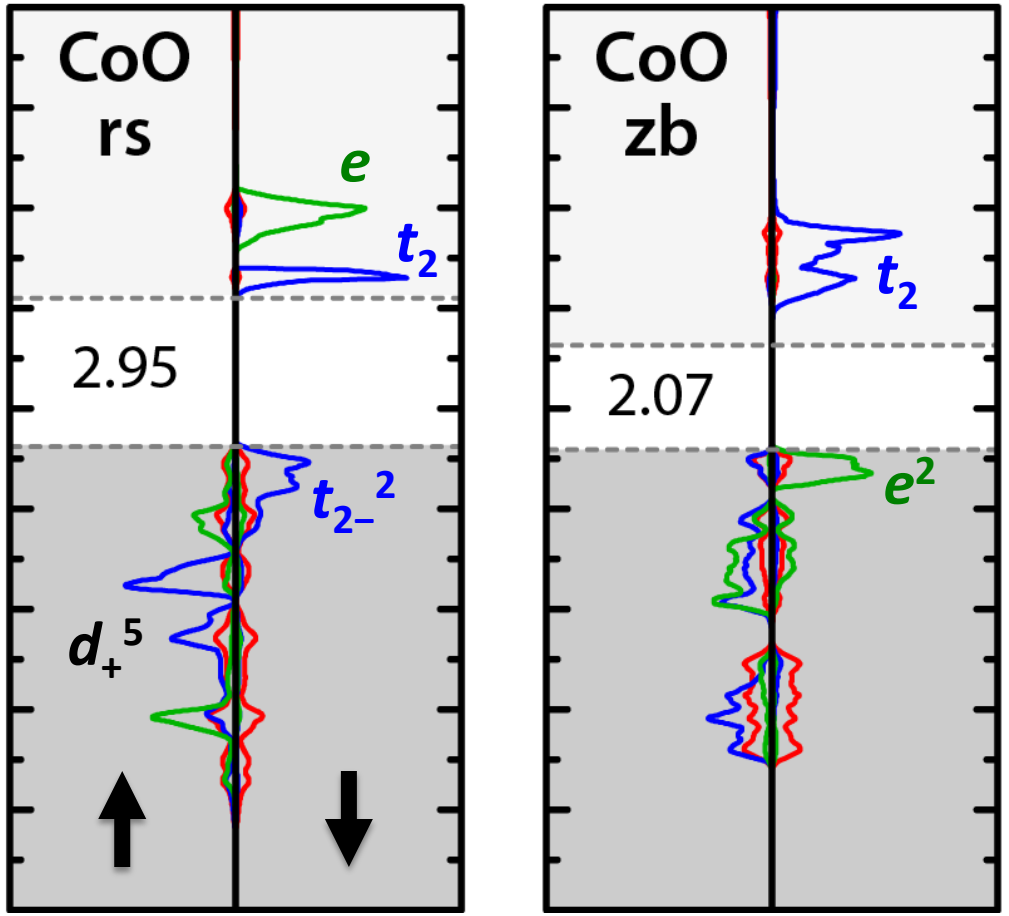

Semiconducting Transition Metal Oxides (Topical Review)
SL, J. Phys. Cond. Mat. **27**, 283203 (2015)

NREL materials Database http://materials.nrel.gov

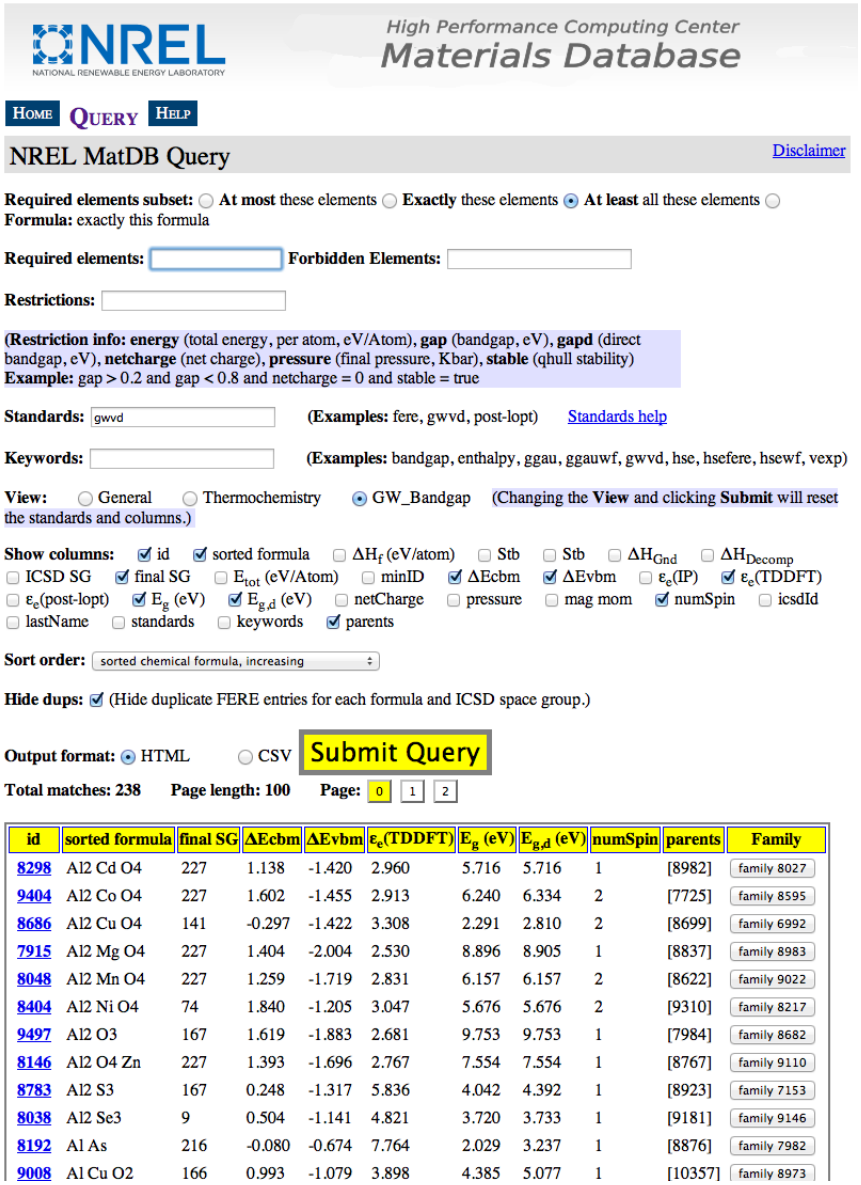

NREL NATIONAL RENEWABLE ENERGY LABORATORY

High Performance Computing Center
Materials Database

HOME QUERY HELP

NREL MatDB Query

Disclaimer

Required elements subset: ○ **At most** these elements ○ **Exactly** these elements ◉ **At least** all these elements ○
Formula: exactly this formula

Required elements: **Forbidden Elements:**

Restrictions:

(Restriction info: energy (total energy, per atom, eV/Atom), **gap** (bandgap, eV), **gapd** (direct bandgap, eV), **netcharge** (net charge), **pressure** (final pressure, Kbar), **stable** (qhull stability)
Example: gap > 0.2 and gap < 0.8 and netcharge = 0 and stable = true

Standards: gwvd **(Examples:** fere, gwvd, post-lopt) Standards help

Keywords: **(Examples:** bandgap, enthalpy, ggau, ggauwf, gwvd, hse, hsefere, hsewf, vexp)

View: ○ General ○ Thermochemistry ◉ GW_Bandgap (Changing the **View** and clicking **Submit** will reset the standards and columns.)

Show columns: ☑ id ☑ sorted formula ☐ ΔH_f (eV/atom) ☐ Stb ☐ Stb ☐ ΔH_{Gnd} ☐ ΔH_{Decomp}
☐ ICSD SG ☑ final SG ☐ E_{tot} (eV/Atom) ☐ minID ☑ ΔEcbm ☑ ΔEvbm ☐ ε_e(IP) ☑ ε_e(TDDFT)
☐ ε_e(post-lopt) ☑ E_g (eV) ☑ $E_{g,d}$ (eV) ☐ netCharge ☐ pressure ☐ mag mom ☑ numSpin ☐ icsdId
☐ lastName ☐ standards ☐ keywords ☑ parents

Sort order: sorted chemical formula, increasing

Hide dups: ☑ (Hide duplicate FERE entries for each formula and ICSD space group.)

Output format: ◉ HTML ○ CSV Submit Query

Total matches: 238 **Page length: 100** **Page:** 0 1 2

id	sorted formula	final SG	ΔEcbm	ΔEvbm	ε_e(TDDFT)	E_g (eV)	$E_{g,d}$ (eV)	numSpin	parents	Family
8298	Al2 Cd O4	227	1.138	-1.420	2.960	5.716	5.716	1	[8982]	family 8027
9404	Al2 Co O4	227	1.602	-1.455	2.913	6.240	6.334	2	[7725]	family 8595
8686	Al2 Cu O4	141	-0.297	-1.422	3.308	2.291	2.810	2	[8699]	family 6992
7915	Al2 Mg O4	227	1.404	-2.004	2.530	8.896	8.905	1	[8837]	family 8983
8048	Al2 Mn O4	227	1.259	-1.719	2.831	6.157	6.157	2	[8622]	family 9022
8404	Al2 Ni O4	74	1.840	-1.205	3.047	5.676	5.676	2	[9310]	family 8217
9497	Al2 O3	167	1.619	-1.883	2.681	9.753	9.753	1	[7984]	family 8682
8146	Al2 O4 Zn	227	1.393	-1.696	2.767	7.554	7.554	1	[8767]	family 9110
8783	Al2 S3	167	0.248	-1.317	5.836	4.042	4.392	1	[8923]	family 7153
8038	Al2 Se3	9	0.504	-1.141	4.821	3.720	3.733	1	[9181]	family 9146
8192	Al As	216	-0.080	-0.674	7.764	2.029	3.237	1	[8876]	family 7982
9008	Al Cu O2	166	0.993	-1.079	3.898	4.385	5.077	1	[10357]	family 8973

DFT level (atomic structure and total energy)

V. Stevanovic

about 20,000 crystalline ordered materials

- Repository of atomic and magnetic structures
- Thermochemistry and stability

GW level (electronic structure)

about 300 semiconducting and insulating materials

- Limited up to 20-30 atoms/cell
- Mostly oxides, chalcogenides, nitrides
- Group 2-15 cations (plus few Li, Na, K)
- Including 3d transition metals and La (4d/5d planned)
- Low energy AFM magnetic configurations
- Polymorphism for II-VI

Supercell defect calculations

Defect equilibrium is determined by defect formation enthalpy

$$c_D = s \cdot \exp^{-\Delta H_D / kT}$$

Compound stoichiometry
Doping and electrical properties
Defect levels, recombination centers

Defect formation energy

$$\Delta H_{\text{ref}} = [E_{\text{tot}}^{D,q} - E_{\text{tot}}^{Host}] + q(E_{\text{VBM}} + \Delta E_{\text{F}}) + \sum_a n_a(\mu_a^0 + \Delta\mu_a)$$

supercell energies | electron reservoir | atomic reservoir

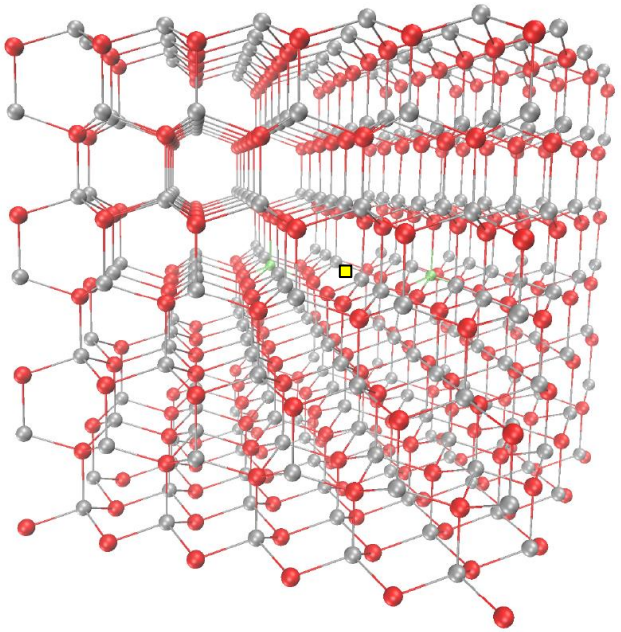

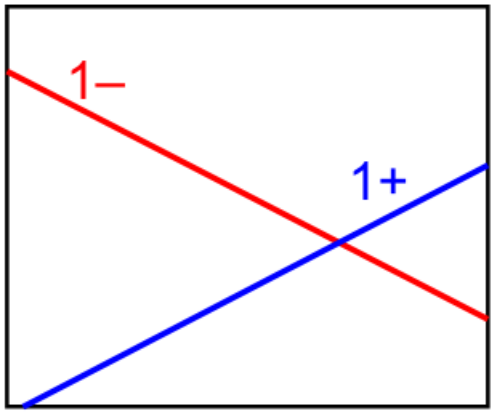

VBM ΔE_F CBM

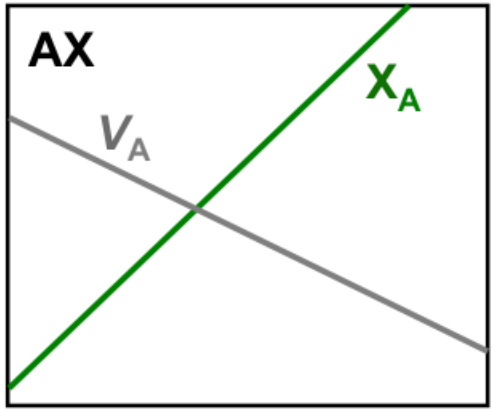

$\Delta\mu_X$

$\Delta\mu_A = 0$ (A metal)

$\Delta\mu_X = 0$ (elem. X)

Supercell corrections vs. finite-size scaling

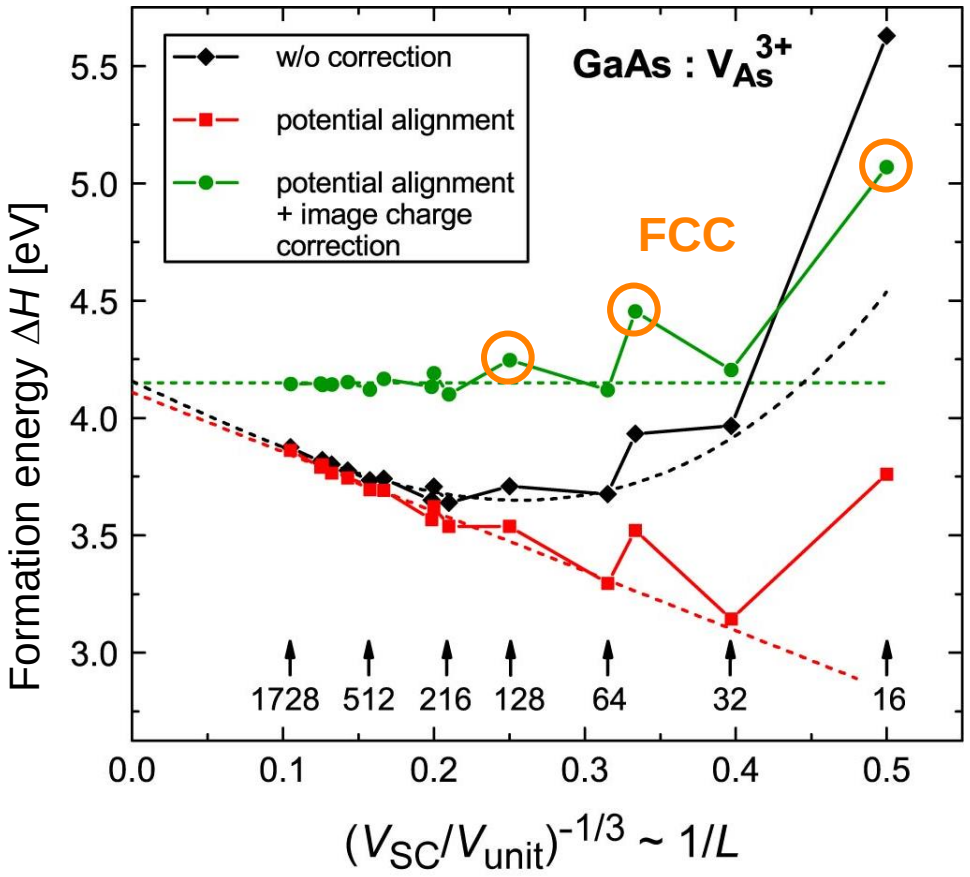

Finite-size scaling

$\Delta H(L)=\Delta H(\infty) + \gamma_1/L + \gamma_3/L^3$

$\Delta H(L)=\Delta H(\infty) + \gamma_1/L$

$\Delta H(L)=\Delta H(\infty)$

Conclusions

- image charge + pot. alignment correction give accurate ΔH
- Avoid FCC symmetries!
- Simple but accurate corrections available

S. Lany, A. Zunger, Phys. Rev. B **78**, 235104 (2008); Modelling Simul. Mater. Sci. Eng. **17** 084002 (2009)

C. Freysoldt, J. Neugebauer, C.G. van de Walle, Phys. Rev. Lett. **102**, 016402 (2009)

Band edge shifts from GW quasi-particle calculations

- Semiconductor materials:
  Cu_3N, Zn_3N_2, AlN, Cu_2O, ZnO, Al_2O_3

- Projector augmented wave implementation of GW in VASP
  [Shishkin & Kresse, PRB 74, 035101 (2006)]

- GW corrected defect formation energies for
  GGA+U: $U_{\text{Cu-d}} = 5$, $U_{\text{Zn-d}} = 6$ eV
  HSE06: standard parameter α = 0.25

- Non-local Fock exchange in hybrid functional

$$V_{nl}(\mathbf{r},\mathbf{r}') = -\alpha \sum_i \frac{\psi_i^*(\mathbf{r}')\psi_i(\mathbf{r})}{|\mathbf{r}-\mathbf{r}'|}\operatorname{erfc}(\mu|\mathbf{r}-\mathbf{r}'|)$$

- GW self-energy

$$\Sigma(\mathbf{r},\mathbf{r}',\omega) = \frac{i}{4\pi}\int_{-\infty}^{\infty} e^{i\omega'\delta} G(\mathbf{r},\mathbf{r}',\omega+\omega')W(\mathbf{r},\mathbf{r}',\omega')d\omega'$$

Example: Cu_2O

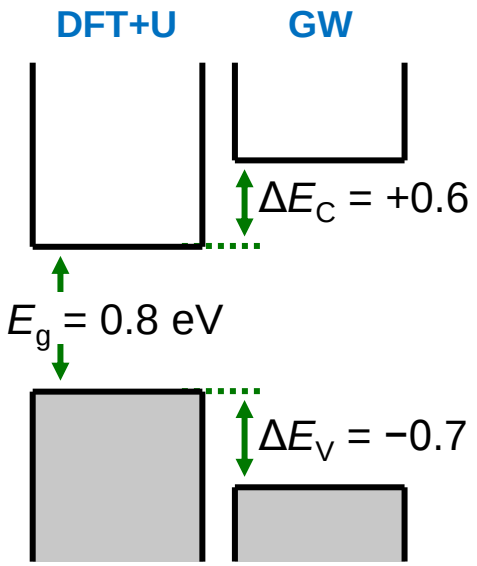

Reference energies for defect formation energies

Defect formation enthalpy for reference states ($E_F = E_{VBM}$; $\mu = \mu^{elem}$)

$$\Delta H_{\text{ref}} = [E_{\text{tot}}^{D,q} - E_{\text{tot}}^{Host}] + q \cdot E_{\text{VBM}}^{\text{ref}} + \sum_a n_a \mu_a^{\text{ref}}$$

- "Band gap problem of DFT" affects E_{VBM}
- **Proposed solution:**
  Anchor ΔH_D at the average potential, use band edge shifts from GW

$$\delta E_{\text{VBM}} = e_{\text{VBM}}^{GW} - e_{\text{VBM}}^{\text{DFT}}$$

- Compare standard DFT (GGA+U) with hybrid functional (HSE06) calculations

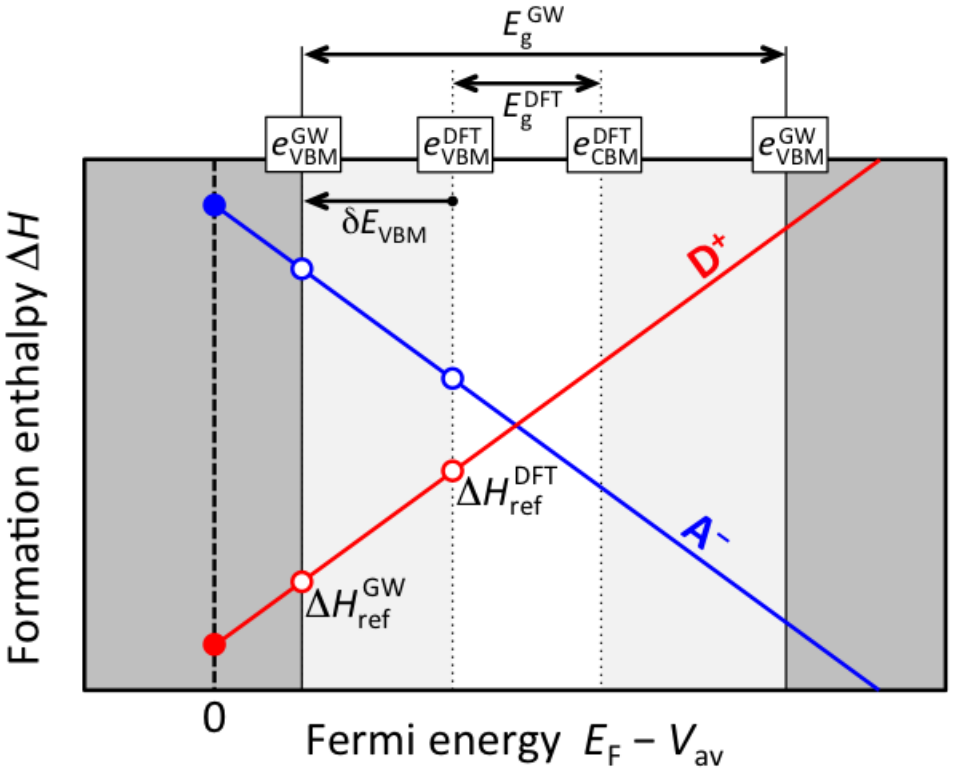

H. Peng, D.O. Scanlon, V. Stevanovic, J. Vidal, G.W. Watson, S. Lany, ***Convergence of density and hybrid functional defect calculations for compound semiconductors***, Phys. Rev. B **88**, 115201 (2013).

Reference energies for defect formation energies

Defect formation enthalpy for reference states ($E_F = E_{VBM}$; $\mu = \mu^{elem}$)

$$\Delta H_{\text{ref}} = [E_{\text{tot}}^{D,q} - E_{\text{tot}}^{Host}] + q \cdot E_{\text{VBM}}^{\text{ref}} + \sum_a n_a \mu_a^{\text{ref}}$$

- Compound formation enthalpies not very accurate in DFT
- Origin: Incomplete error cancellation between compounds and elements
- **Proposed solution:**
  Fitted elemental reference energies (FERE)

  $\delta\mu_a = \mu_a^{\text{FERE}} - \mu_a^{\text{DFT}}$
- RMS error reduced in GGA from 0.24 to 0.07 eV/atom
  Consistency of DFT within cation-anion compounds
- Expected to improve thermodynamic boundary conditions for ΔH_D calculations

$$\Delta H_f^{SC} = E_{\text{tot}}^{SC} - \sum m_a \mu_a^{\text{ref}}$$

Semiconductor compound — Metals Molecules

$$\sum m_a \delta\mu_a = \Delta H_f^{\text{DFT}} - \Delta H_f^{\text{ex}}$$

least square fit for $\delta\mu_a$

Example:

$\Delta H_f(Al_2O_3) = E_{\text{tot}}(Al_2O_3) - 2\mu_{Al} - 3\mu_O$

= −14.9 eV (GGA)

= −17.4 eV (expt.)

= −17.3 eV (FERE)

S. Lany, ***Semiconductor thermochemistry in density functional calculations***, Phys. Rev. B 78, 245207 (2008).

Comparison of density and hybrid functionals

Band gaps

E_g	PBE+U eV	HSE eV	GW eV
Cu_3N	0.8	1.0	1.0
Zn_3N_2	0.2	0.9	1.1
AlN	4.2	5.6	6.4
Cu_2O	0.8	2.0	2.2
ZnO	1.5	2.5	3.5
Al_2O_3	6.3	8.1	9.9

VBM energy

ΔE_{VBM}	PBE+U eV	HSE eV
Cu_3N	−0.4	−0.3
Zn_3N_2	−0.4	−0.1
AlN	−1.3	−0.5
Cu_2O	−0.7	−0.4
ZnO	−1.1	−0.6
Al_2O_3	−1.9	−0.7

Elemental energy

FERE δμ	PBE+U eV	HSE eV
Cu	−0.02	±0.00
Zn	−0.08	+0.24
Al	+0.66	+0.35
N	−0.03	−0.04
O	+0.34	+0.32

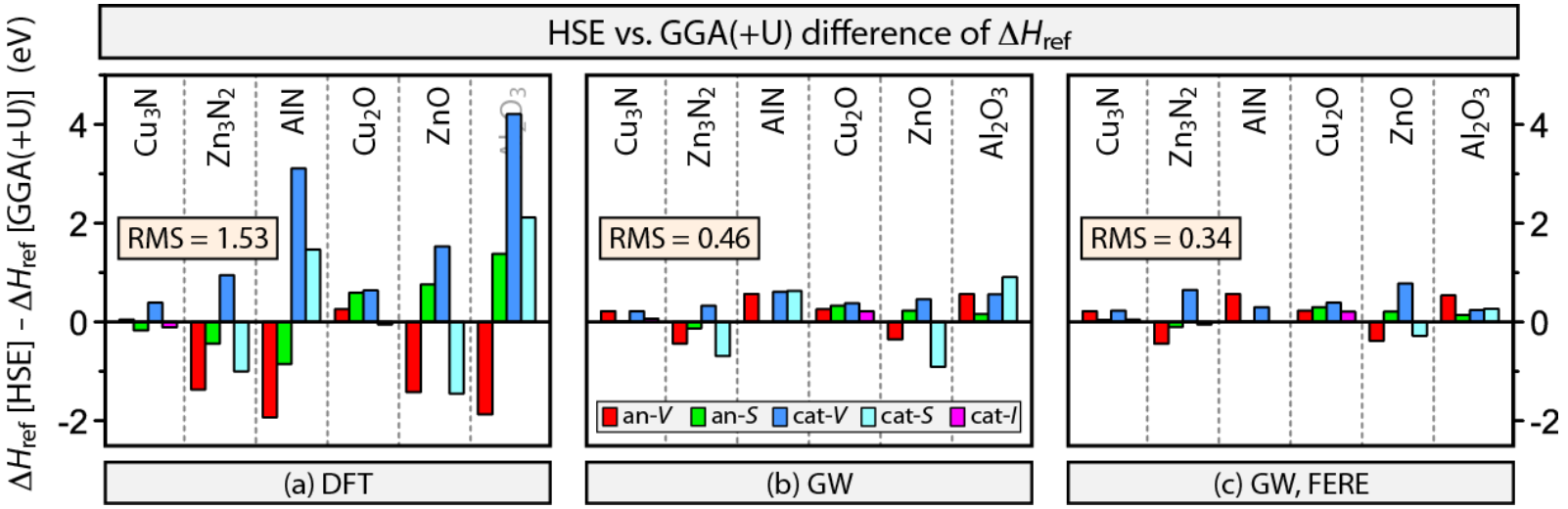

H. Peng, D.O. Scanlon, V. Stevanovic, J. Vidal, G.W. Watson, S. Lany, ***Convergence of density and hybrid functional defect calculations for compound semiconductors***, Phys. Rev. B **88**, 115201 (2013).

Defect equilibria and “defect phase diagrams”

Thermodynamic modeling

Defect formation energy	$\Delta H = \Delta H_{D,q}(\mu, E_F)$
Defect concentration	$c_D \approx N_{site} \times \exp(-\Delta H/kT)$
Electron/hole density	$c_e = \int f_{FD}(E-E_F)\, g(E)\, dE$
Charge neutrality	$-c_e + c_h + \Sigma\,[q \cdot c(D^q)] = 0$
Self-consistent solution	$\Delta H(E_F) \longrightarrow c_D(\Delta H) \longrightarrow E_F$ (cycle)
pO_2 dependence of μ_O	$\Delta\mu_O(T,P_0) = \frac{1}{2}[H_0+\Delta H(T)] - \frac{1}{2}T\cdot[S_0+\Delta S(T)]$
(ideal gas)	$\Delta\mu_O(T,P) = \Delta\mu_O(T,P_0) + \frac{1}{2}kT\ln(P/P_0)$

Temperature dependence of band gap (CBM)

Dopant-defect association / dissociation within law of mass action

K. Biswas and S. Lany, Phys. Rev. B **80**, 115206 (2009)

Example: *n*-type doping in ZnO

Formation energies of dopants, defects and defect pairs

192 atoms supercells, GGA+U, ΔE_V (GW), fitted elemental reference energies (FERE) [1]

$$\Delta H_{D,q}(\mu, E_F) = [E_{D,q} - E_{host}] + [\mu_{host} - \mu_D] + q \cdot E_F$$

Supercell total energies | Atomic chemical potentials | Electron chem. potential

Active players:

Isolated dopants/defects: Ga_{Zn}^{1+}, V_{Zn}^{2-}, $V_O^{0/2+}$

Pairs and complexes: $(Ga_{Zn} - V_{Zn})^{1-}$

$(2Ga_{Zn} - V_{Zn})^{0}$

Law of mass action

$[(Ga_{Zn}\text{-}V_{Zn})] = [Ga_{Zn}] \times [V_{Zn}] \times \exp(-E_{b1}/kT)$

$E_{b1} = -1.1$ eV

$[(2Ga_{Zn}\text{-}V_{Zn})] = [Ga_{Zn}]^2 \times [V_{Zn}] \times \exp(-E_{b2}/kT)$

$E_{b2} = -1.8$ eV

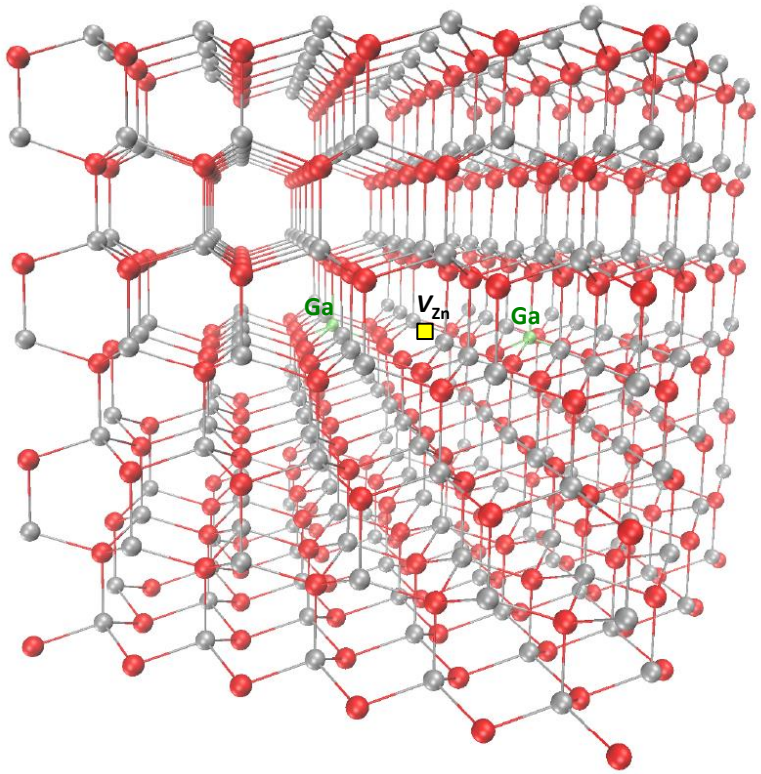

Solubility limit of Al, Ga, In in ZnO

Limiting competing oxide-phases: Al_2ZnO_4, Ga_2ZnO_4, In_2O_3

Equilibrium of ZnO: $\Delta\mu_{Zn} + \Delta\mu_O = \Delta H_f(ZnO)$

dopant: $2\Delta\mu_{Al} + \Delta\mu_{Zn} + 4\,\Delta\mu_O = \Delta H_f(Al_2ZnO_4)$

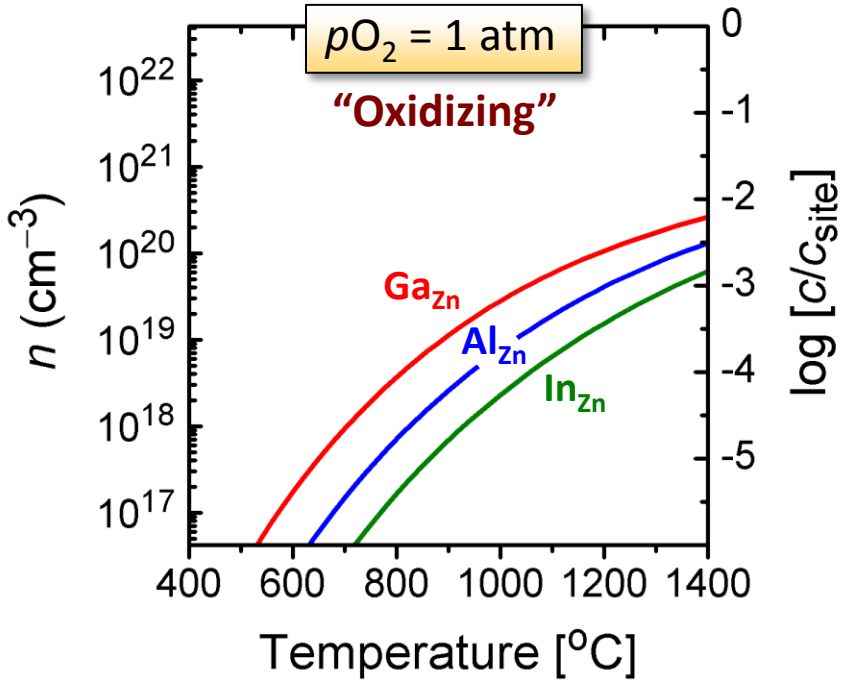

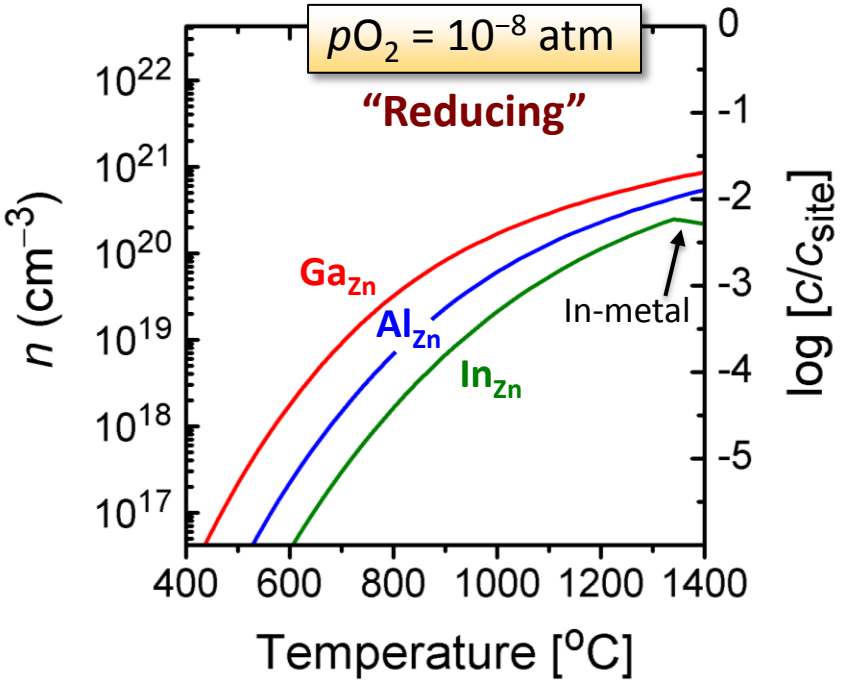

Solubility in the per cent range only at high temperatures above 1000°C

At equilibrium conditions, moderate compensation (up to ~10%)

Influence of band edge shift and defect pairs

Constrained equilibrium: $c(Ga_{Zn})$ is constant, but compensation by V_{Zn} is equilibrated

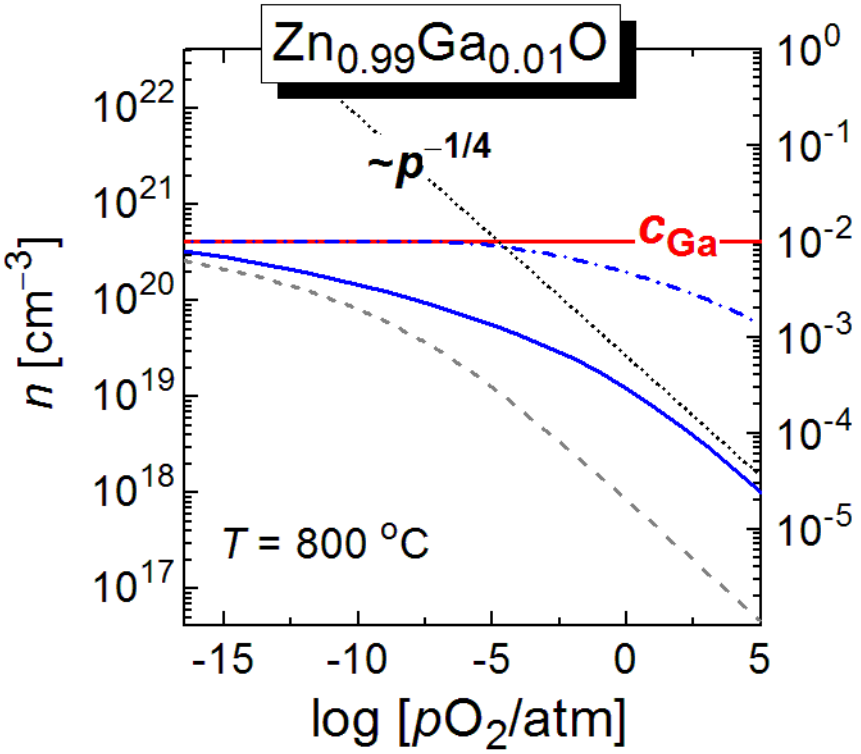

- – – – – “2007” model
- —·—·— incl. GW band edge shifts increases *n*
- ——— incl. defect pair binding reduces *n*

Large, counteracting effects

Strong compensation at high (supersaturated) Ga dopant concentrations, most compensating defects (V_{Zn}) occur as fully passivated complexes ($2Ga_{Zn}$ - V_{Zn})

Temperature dependence of *n*

Constrained equilibrium
(2% cat. Ga)

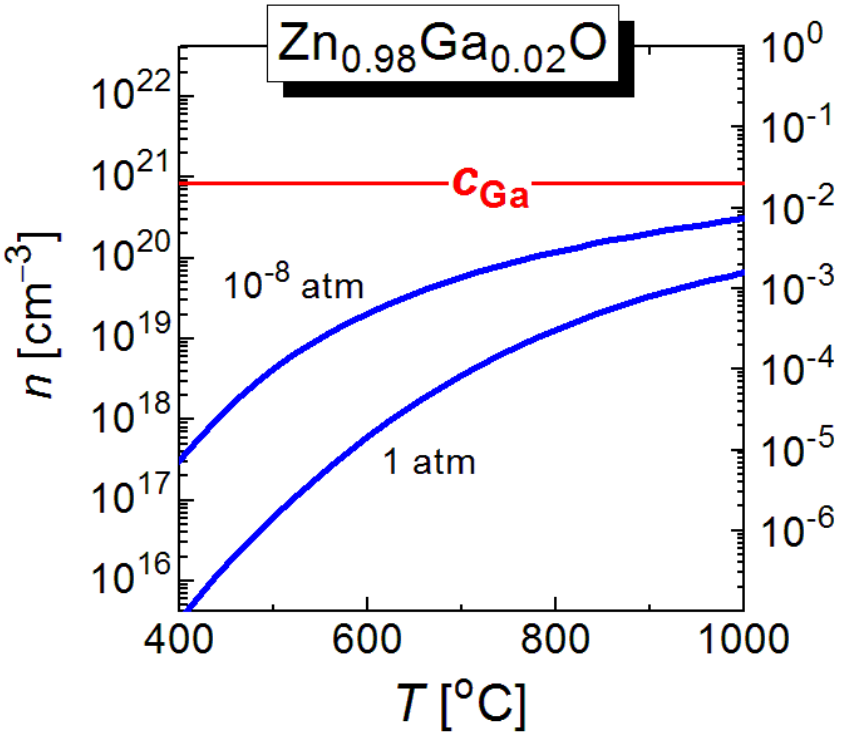

Why does *n* increase with *T*?

- reduction of $\Delta\mu_O$ with T at given pO_2
  respective increase of $\Delta\mu_{Zn}$ and $\Delta H_D(V_{Zn})$

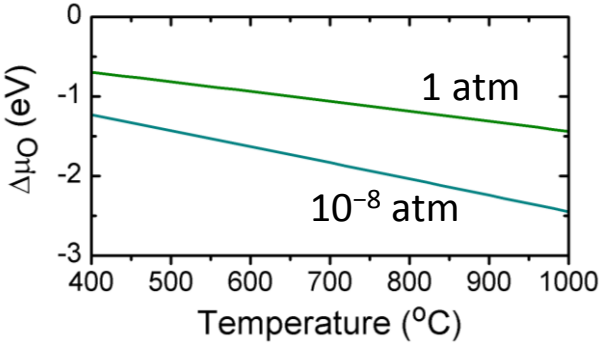

- reduction of band gap (E_{CBM})
  $\Delta E_g/\Delta T$ = 0.6 meV/K

F.J. Manjon et al, Sol. Stat. Comm. **128**, 35 (2003)

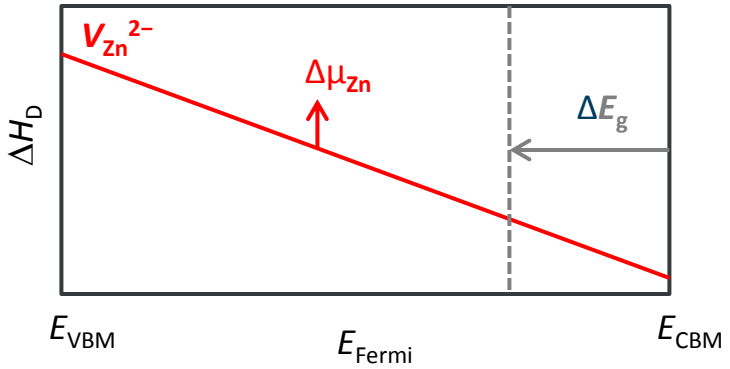

Comparison with as-grown doped ZnO

Highly doped ZnO:Al, ZnO:Ga only as thin-films

Typical literature growth methods and results

- PLD, Sputtering, MOCVD
- $T_{sub} \approx$ 200-300 °C
- $pO_2 \leq 10^{-6}$ atm
- c(Al,Ga) up to 5% cat.
- $n \approx 10^{21}$ cm^{-3}

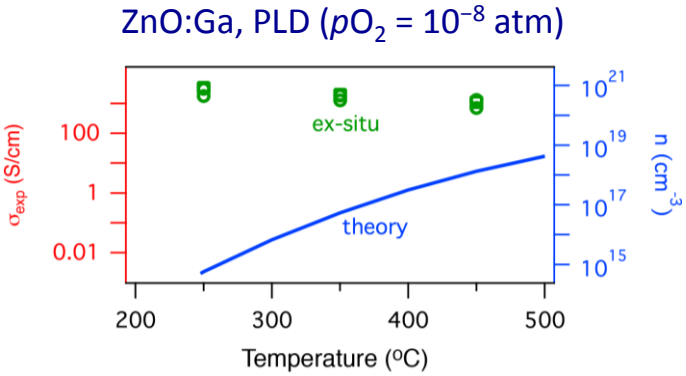

As-grown films have much higher ***dopant*** concentration than predicted ***equilibrium solubility*** limit
(not so surprising)

As-grown films have much higher ***carrier*** concentration than predicted for ***constrained equilibrium*** at moderate *T*
(surprising?)

Temperature dependence of *n*

In-situ measurement of conductivity (NU): Direct monitoring of the equilibration process

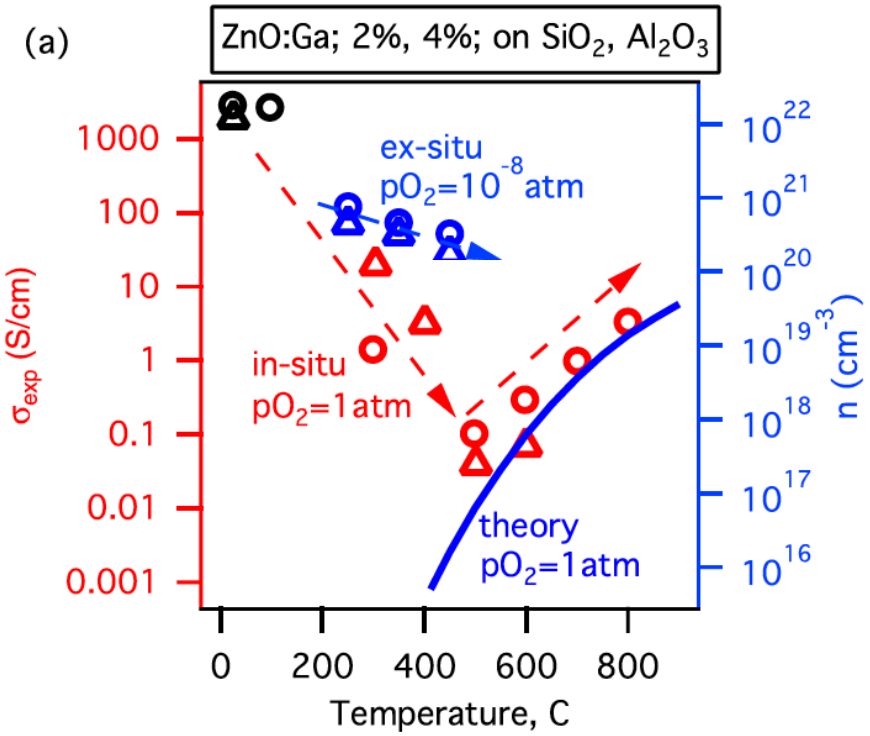

Mobility

initially μ = 20 cm^2/Vs at room temperature

in-situ lower μ = 1 cm^2/Vs (plot scaling)

- Conductivity decreases 3 orders of magnitude already at 300°C (1 atm pO_2)
- Minimum of σ around 500°C
- Conductivity increase at higher *T* in agreement with prediction

pO_2 dependence of n

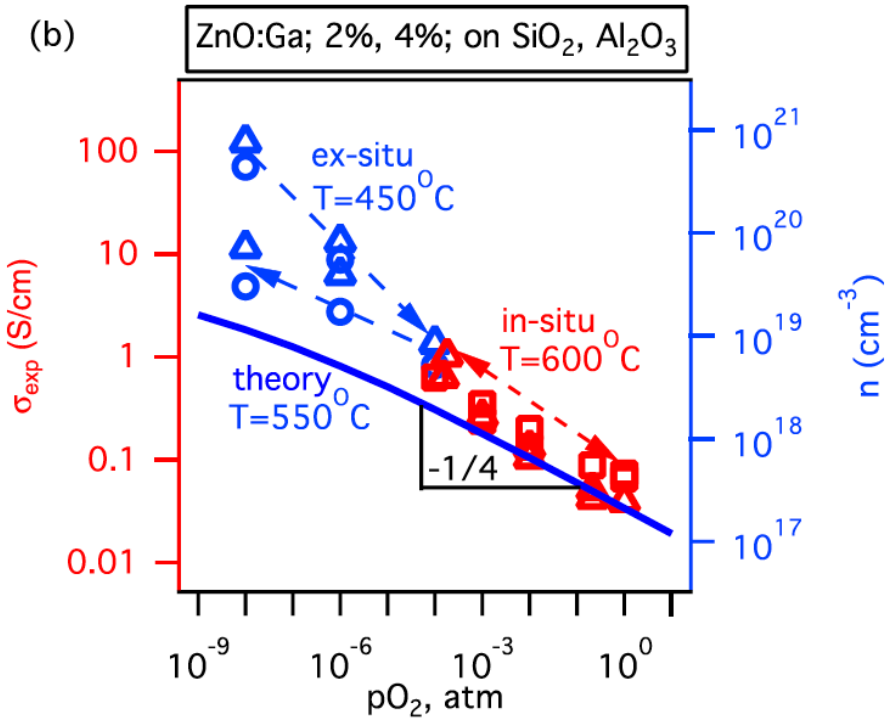

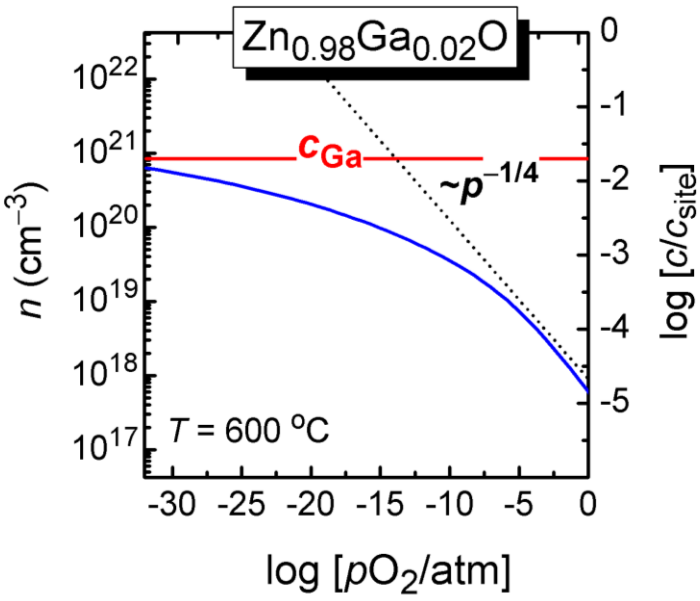

- Fast equilibration at high pO_2 (1 atm) around 500°C
- Slow equilibration at low pO_2 (10^{-8} atm)
- Observation of expected $p^{-1/4}$ dependence at high pO_2

A. Zakutayev, N.H. Perry, T.O. Mason, D.S. Ginley, S. Lany, ***Non-equilibrium origin of high electrical conductivity in gallium zinc oxide thin films***, Appl. Phys. Lett. **103**, 232106 (2013).

Compensating defects in Ga_2O_3 polymorphs

Ga_2O_3 polymorphs	β (GS)	α (Al_2O_3)	δ (In_2O_3)
$E - E_{GS}$ (meV/at.) - DFT	0	+28	+30
E_g (eV) - GW	4.96	5.28	4.89

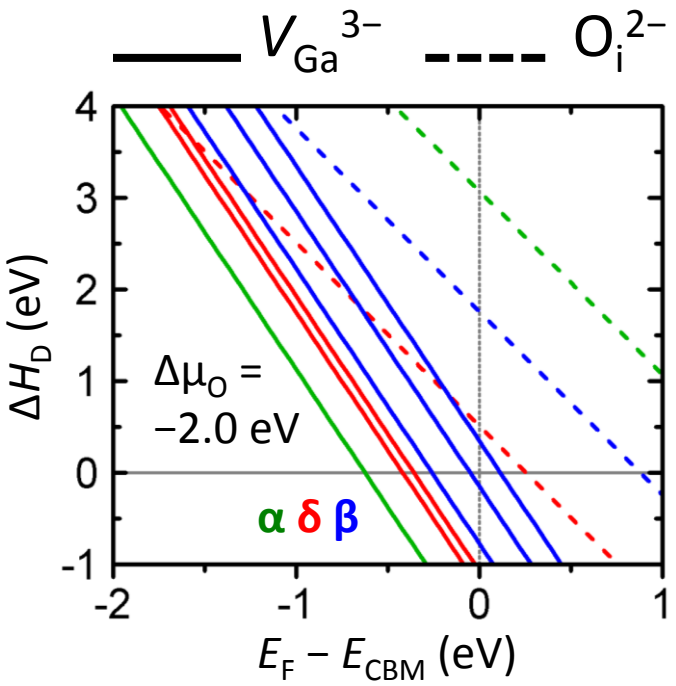

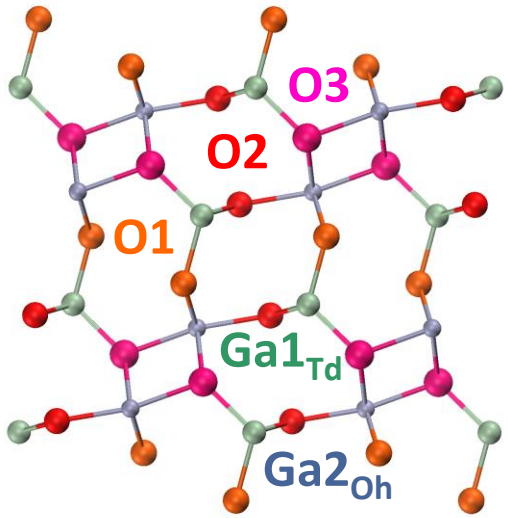

5 non-equivalent sites in β-Ga_2O_3

- Similar band gaps in all polymorphs
- Ga vacancies are the dominant defect (unlike O_i in In_2O_3)
- PAS experiments [Korhonen et al. APL **106**, 242103 (20150]
- Highest ΔH_D in ground state β-Ga_2O_3

Which dopant releases free carriers?

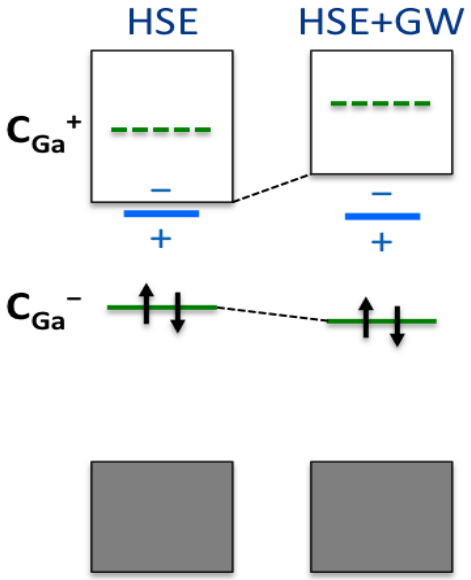

	E_{Oh-Td} (eV)	ε(+/−) HSE	ε(+/−) GW
C_{Td}	+1.15	−0.04	−0.81
Si_{Td}	+0.73	+1.19	+0.80
Ge_{Td}	+0.11	+0.56	−0.14
Sn_{Td}		+0.27	−0.41
Sn_{Oh}	−1.10	+0.58	−0.19

DX center

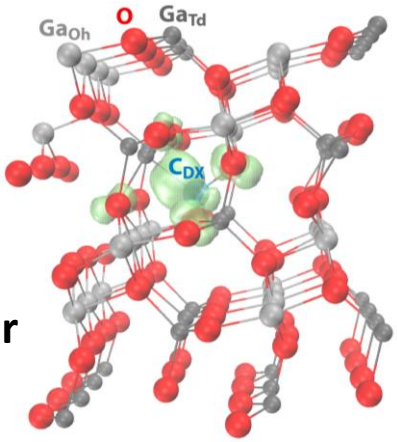

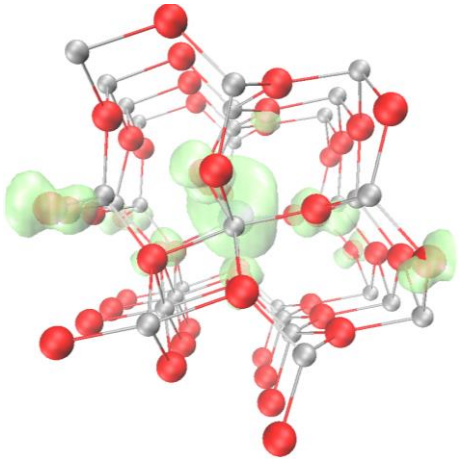

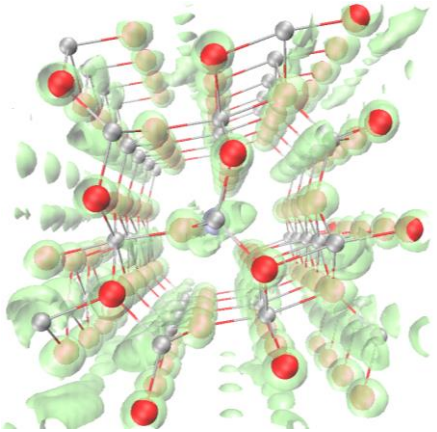

C_{Ga1}: deep level ☹

Sn_{Ga2}: so-so

Si_{Ga1}: shallow level ☺

Dopant – defect interactions

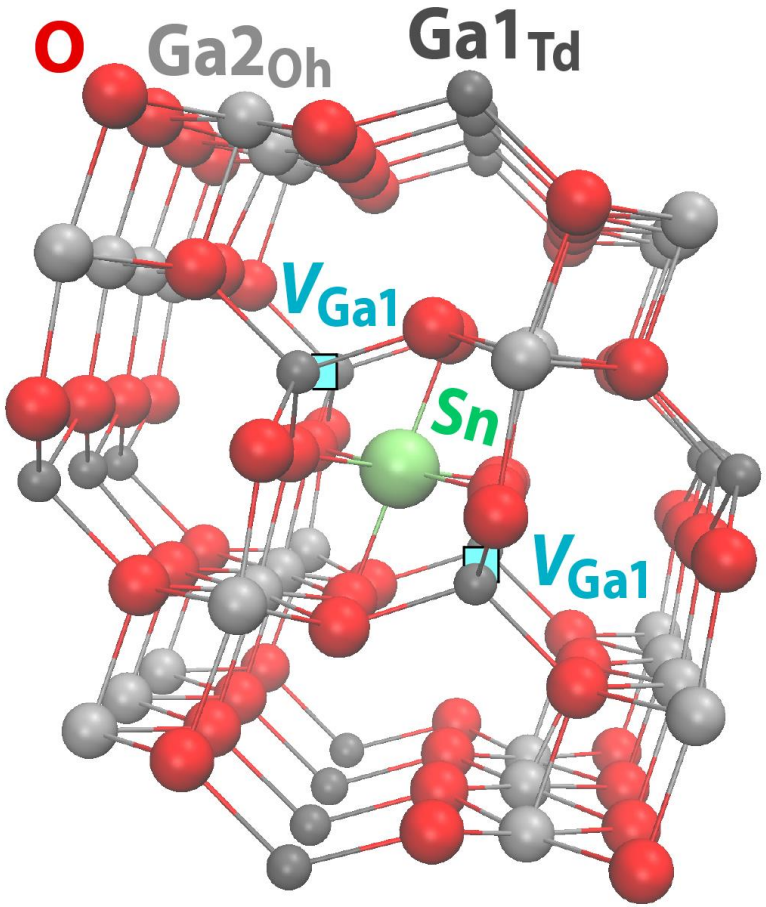

- **Supercells**
  Standard DFT (GGA)
  160 atom cells for defect pairs
- **Site-preference**
  Sn_{Ga} @ $Ga2_{Oh}$
- **"Split-vacancy"**
  V_{Ga} -> (Ga_i + 2V_{Ga1})
- **Defect pairs**
  Sn_{Ga1} +V_{Ga} -> (Sn_i + 2V_{Ga1})
  ΔE_b = –1.2 eV wrt Sn_{Ga2}
  (Sn_i + 2V_{Ga1}) + Sn_{Ga2}
  ΔE_b = –0.6 eV
  (Sn_i + 2V_{Ga1}) + 2Sn_{Ga2}
  ΔE_b = –0.2 eV

Defect equilibria

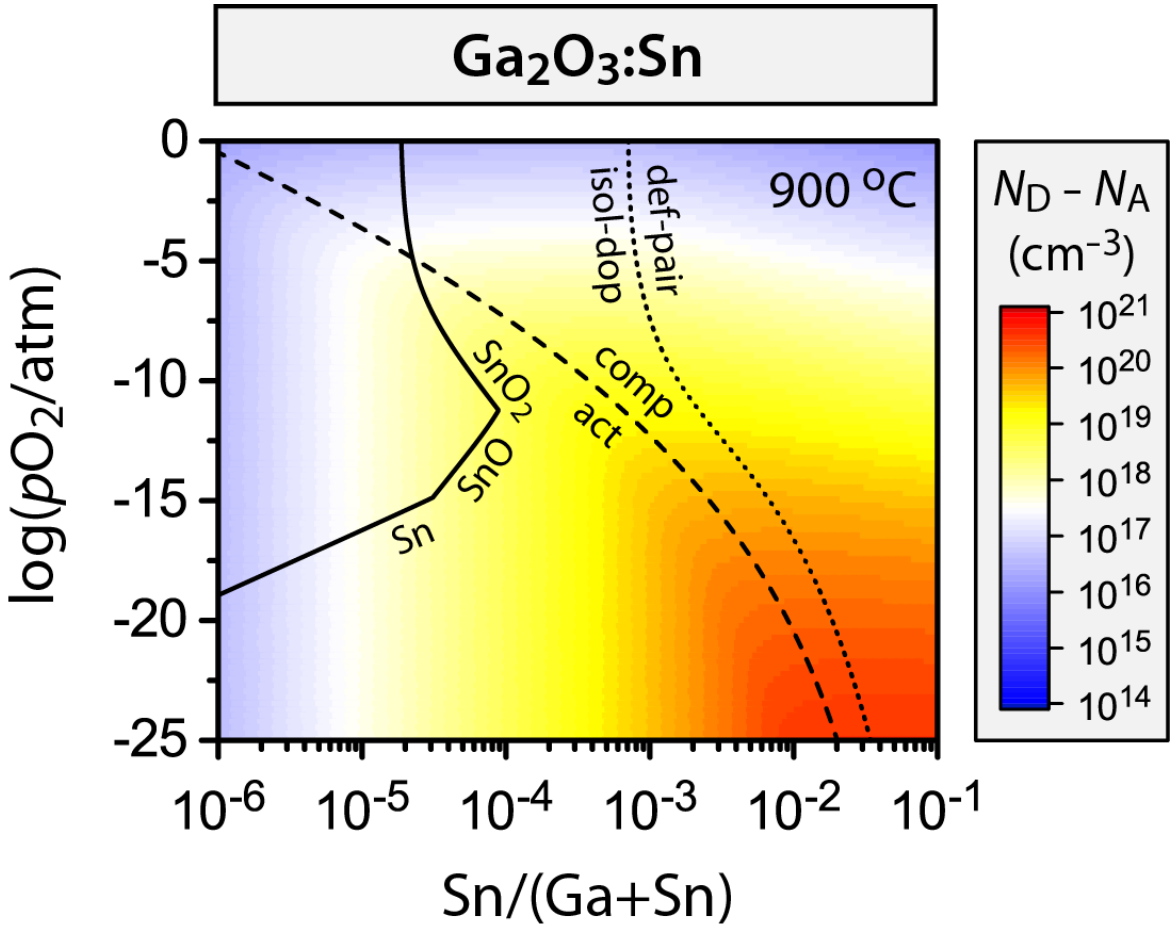

- Net doping ($N_D - N_A$) vs. pO_2 and c(Sn)
- Solubility limits
- Activated vs. compensated doping
- Isolated defects vs. defect-pairs

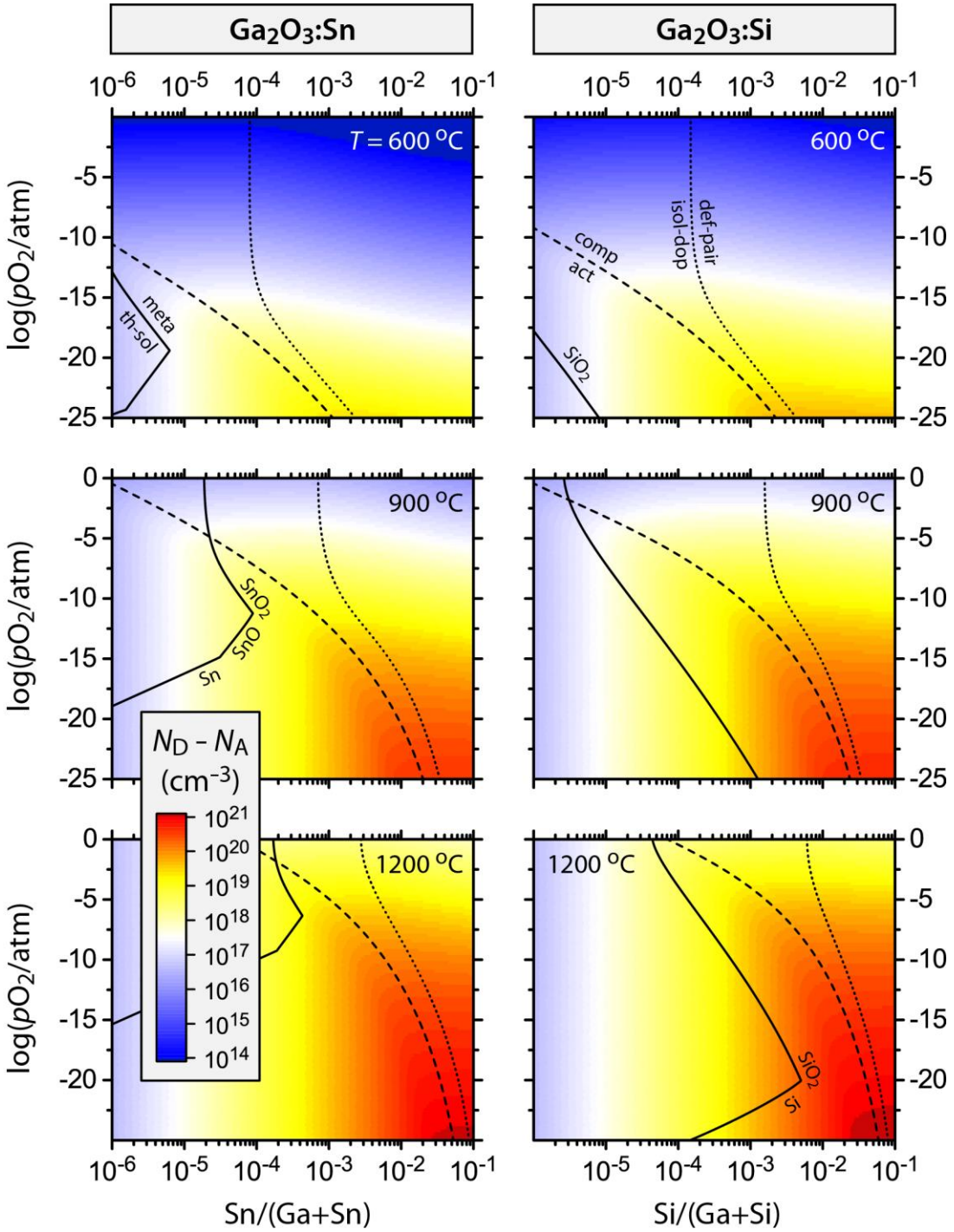

Sn vs Si and temperature trends

Dopant choice

- Si slightly less compensated than Sn

Increasing *T* causes

- Higher solubility limits
- Lower compensation ratio
- Higher limit of dopant conc.
- Higher $N_D - N_A$

Optimizing experimental conditions

DPD: High T, low pO_2, optimal dopant conc.

Thermodynamics: High pGa_2O causes material loss

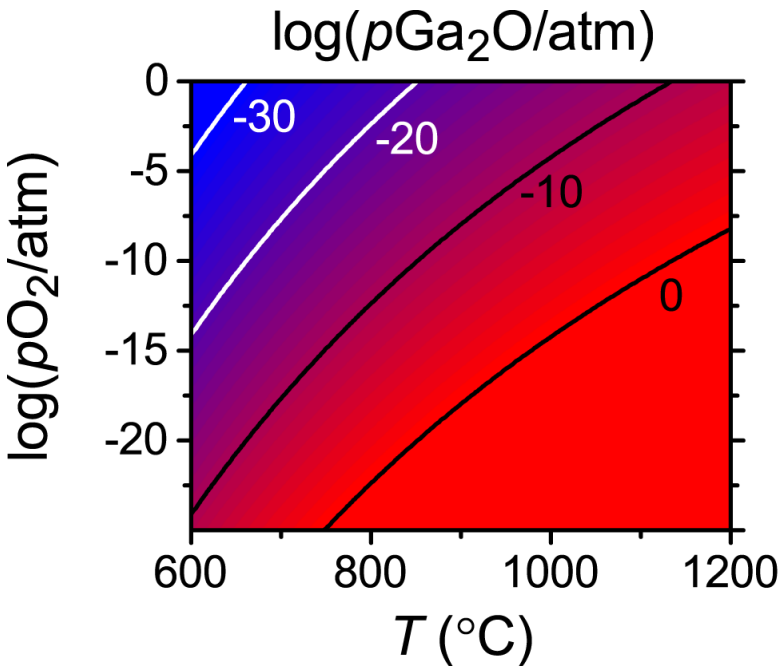

T (°C)	log(pO_2) (atm)	$N_D - N_A$ (10^{20} cm^{-3})	Si/Si+Ga (10^{20} cm^{-3})	in Si cat%
600	-29.2	1.4	11.0	2.9%
700	-22.6	1.0	6.9	1.8%
800	-17.4	0.8	4.5	1.2%
900	-13.0	0.6	3.0	0.8%
1000	-9.2	0.4	2.2	0.6%

Maximal doping: Lower T, optimize pO_2 and Si conc.

Disordered multinary compounds

Multinary compounds: Cu_2ZnSnS_4 (CZTS) and Cu_2SnS_3 (CTS)

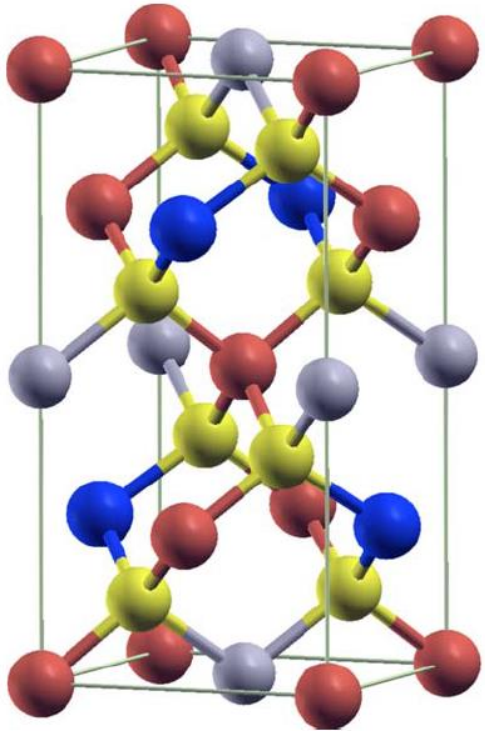

Cu, Sn

Cu, **Zn**

Sn, **Cu**

Zn, **Cu**

Cu, Sn

A. Nagoya, PRB **79**, 115126 (2009)

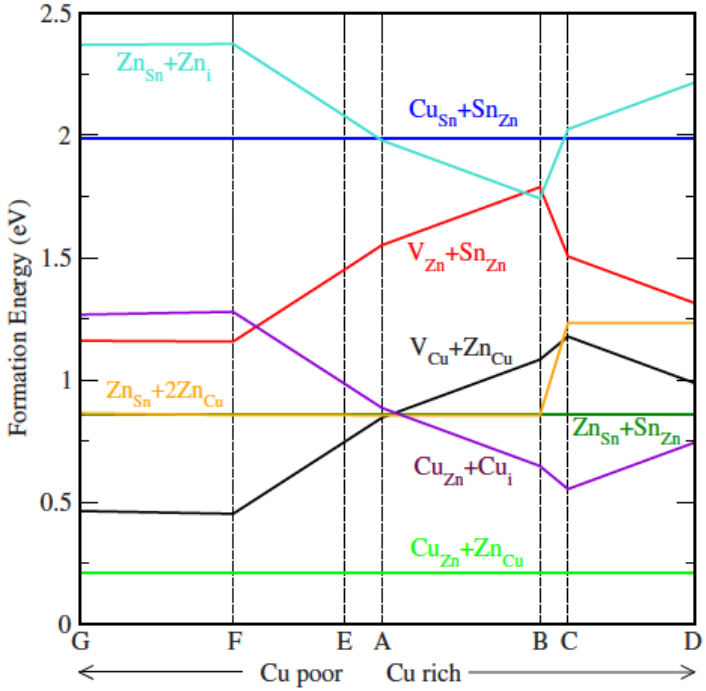

S. Chen et al., PRB **81**, 245204 (2010)

- Experiment: Order – disorder phenomena
- Theory: Cu_{Zn} – Zn_{Cu} defect pair
- Description beyond the defect model?

Model Hamiltonian: CZTS and Cu_2SnS_3 (CTS)

S-$Cu_iSn_jZn_{4-i-j}$ motifs

S-Cu3Sn

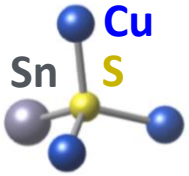

S-Cu2Sn2

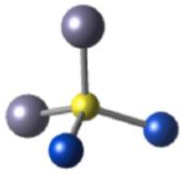

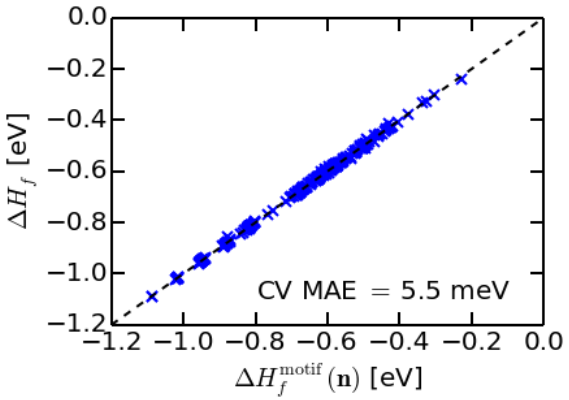

$$\mathrm{D}_f H = 2\sum_{(i,j)} e_f(i,j)\, n(i,j)$$

j \ i	0	1	2	3	4
0	-1.083	-0.914	-0.679	-0.404	-0.238
1	-0.880	-0.790	-0.663	-0.492	
2	-0.565	-0.563	-0.463		
3	-0.379	-0.254			
4	-0.026				

S-$CuSnZn_2$
S-Cu_2SnZn
S-Cu_3Sn
S-Cu_2Sn_2

- Motif based Hamiltonian emphasizes local order and octet rule
- Good fit even thought long range order effects are excluded
- Simple Hamiltonian allows efficient Monte-Carlo simulations

Entropy-driven clustering in CTS

Monte Carlo simulations

ordered disordered

CTS

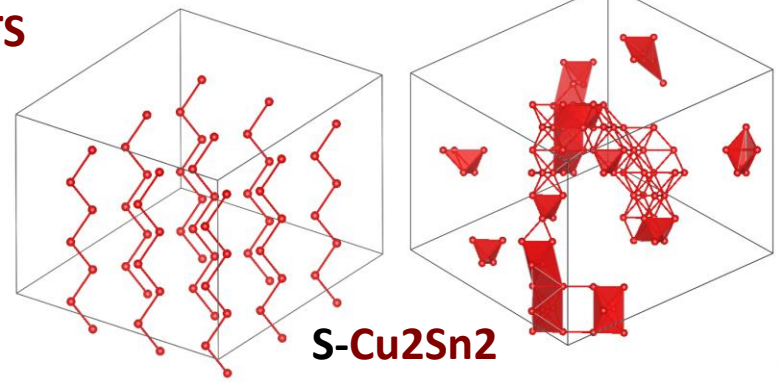

S-Cu2Sn2

S-Cu3Sn1

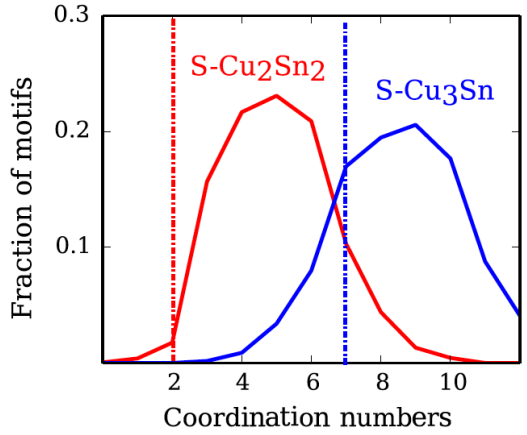

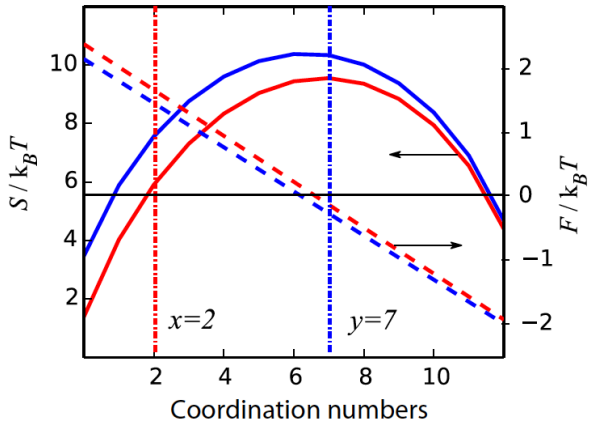

- Disorder induced clustering
- Weakly temperature dependent

P. Zawadzki, A. Zakutayev, and S. Lany, ***Entropy-driven clustering in tetrahedrally bonded multinary materials***, Phys. Rev. Appl. **3**, 034007 (2015).

Order-disorder transition in CZTS

Monte Carlo simulations

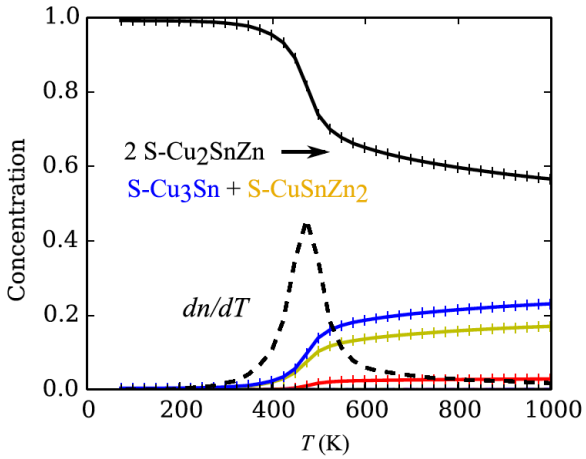

S-Cu_2SnZn
S-Cu_2Sn
S-$CuSnZn_2$

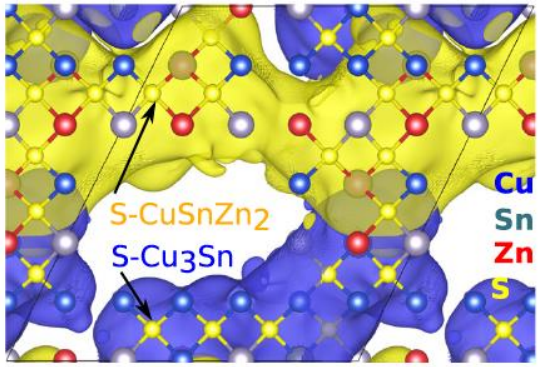

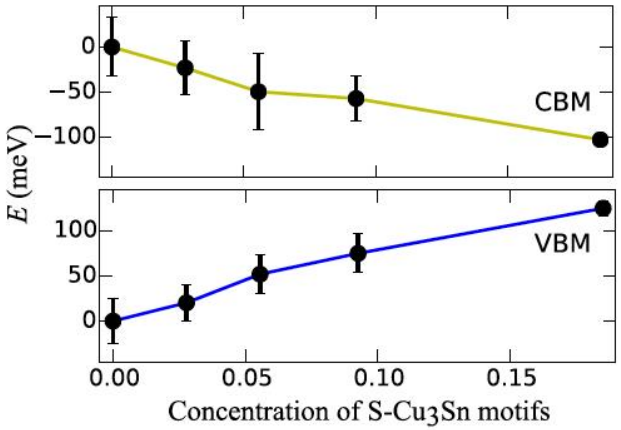

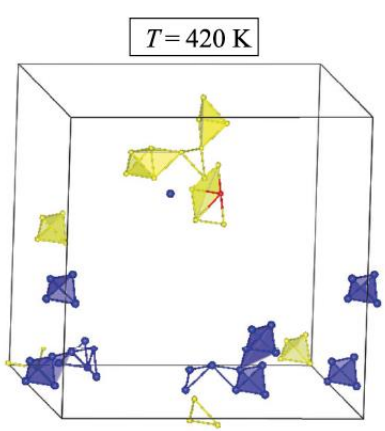

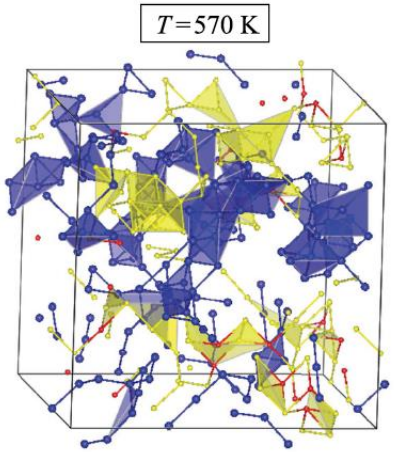

- Entropy driven clustering amplifies potential fluctuations

P. Zawadzki, A. Zakutayev, and S. Lany, ***Entropy-driven clustering in tetrahedrally bonded multinary materials***, Phys. Rev. Appl. **3**, 034007 (2015).

Implication for point defects: “Extended anti-sites”

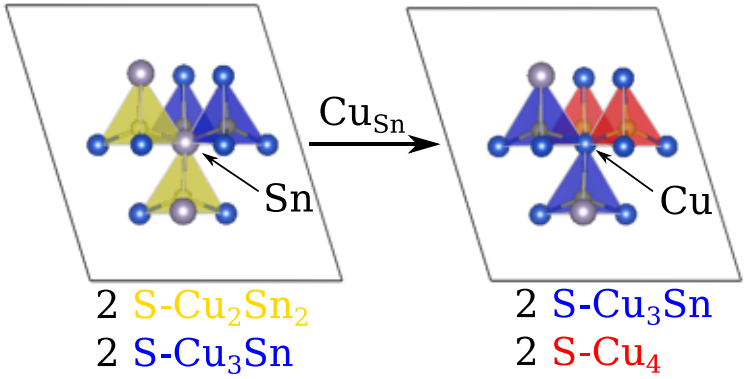

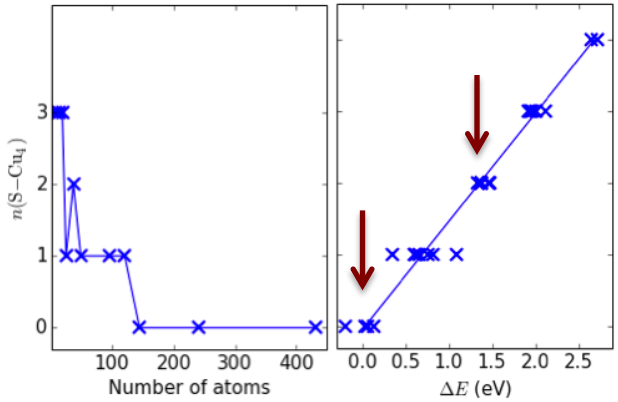

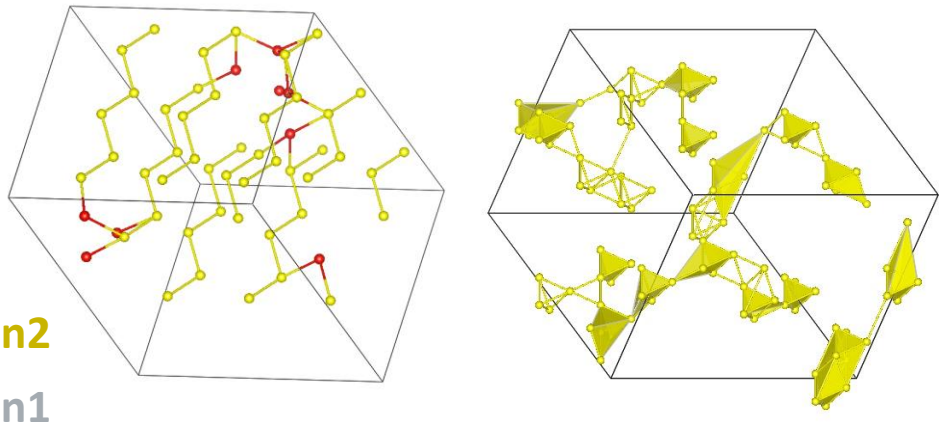

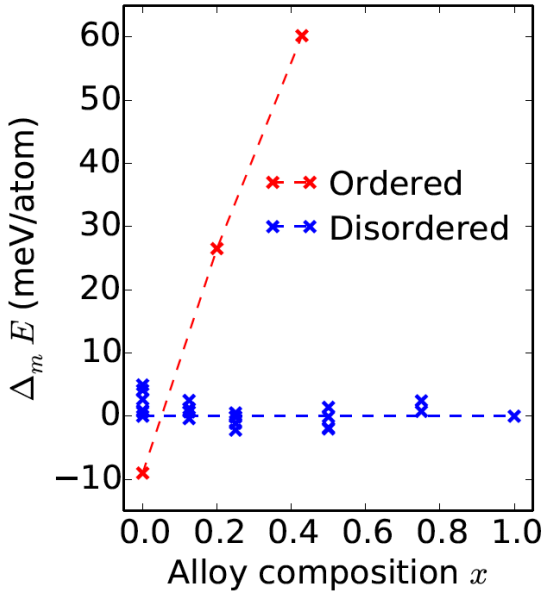

- Formation energy of Cu_{Sn} reduced by 1.5 eV in disordered CTS
- Point defect model in ordered crystal does not capture energetics of off-stoichiometry

P. Zawadzki, A. Zakutayev, S. Lany, ***Extended antisite defects in tetrahedrally bonded semiconductors***, Phys. Rev. B **92**, 201204(R) (2015)

Cation ordering in $ZnSnN_2$

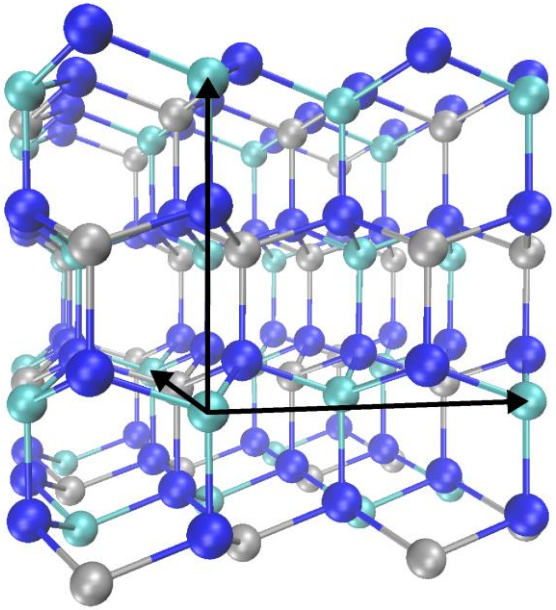

Crystal structure of ordered $ZnSnN_2$ (ZTN)

- Orthorhombic (ORC) cell is supercell of Wurtzite (WZ)
- All N atoms coordinated by 2 Zn and 2 Sn

Zn2Sn2

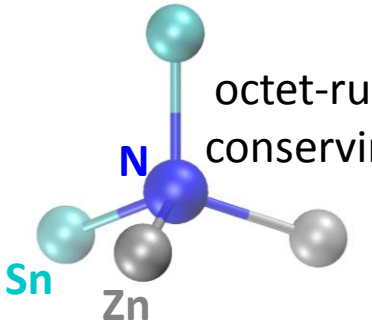

octet-rule conserving

Zn3Sn1

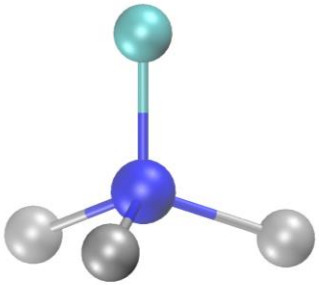

Sn4

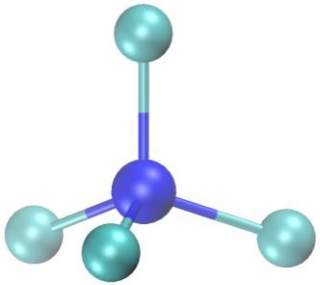

$$\Delta H = \sum_i n(i)\, e(i)$$

ZTN disorder: Phase transition and energies

Energies (DFT)

- Disordered octet-conserving: Essentially degenerate, ΔH = 0.5 meV/atom, occurs at any temperature
- Average energy is linear in concentration $x_{31} = x_{13}$ of Zn3Sn1 motifs

Disorder vs temperature (model H)

- Ordered ground state: only Zn2Sn2 motifs (octet)
- Around 2000°C transition to phase with 40% of Zn3Sn1+Zn1Sn3 motifs
- Zn4 and Sn4 stay below 1%

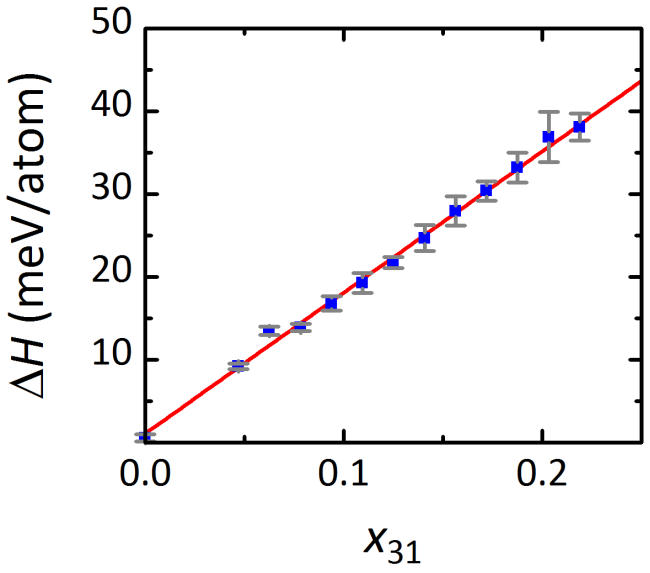

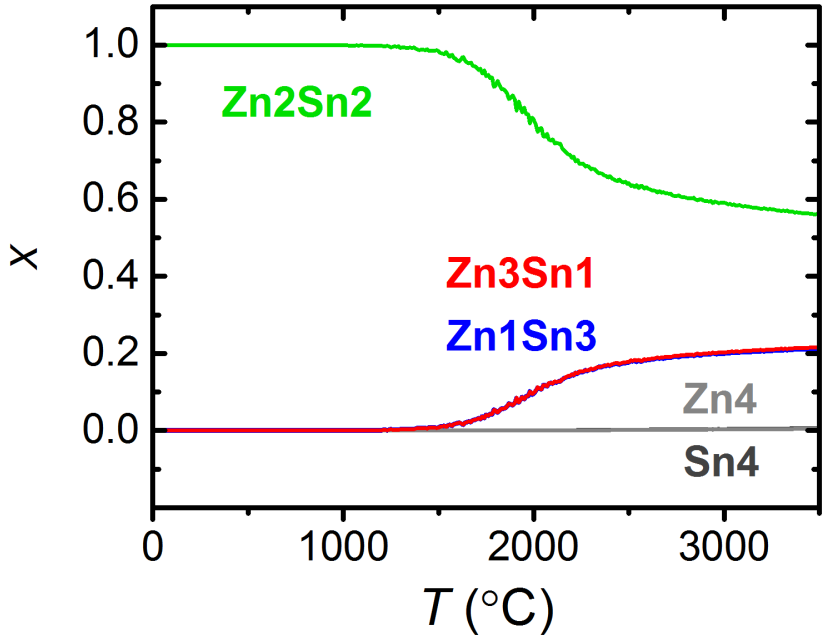

Band gap calculations

Approach

- Need to avoid "DFT band gap error"
- Full-fledged GW calculations not feasible for supercells of disordered ZTN
- Use "single-shot" hybrid functional, plus on-site potential *U* for Zn-d
- Fitting to GW calculation for $ZnSnN_2$, Zn_3N_2, and Sn_3N_4

$$e_n^{GW} = e_n^{DFT} + \mathrm{Re}\left\langle \psi_n^{DFT} \middle| \Sigma(e_n^{GW}) - V_{xc}^{DFT} \middle| \psi_n^{DFT} \right\rangle$$

Screening in GW: $W = W(\mathbf{r},\mathbf{r}',\omega)$

Hybrid functional: scaling by $\alpha < 1$

Fit result: $\alpha = 0.14$, $U_{Zn\text{-}d} = 4$ eV

E_g within 0.1 eV,
VBM, CBM, Zn-d within 0.2 eV

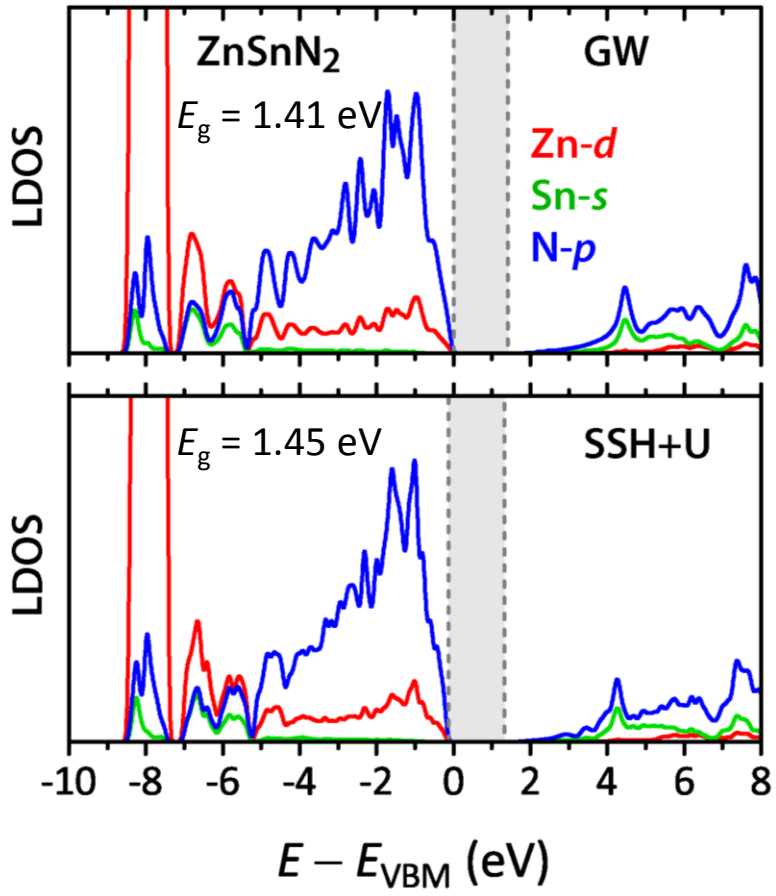

Disorder effects on electronic structure

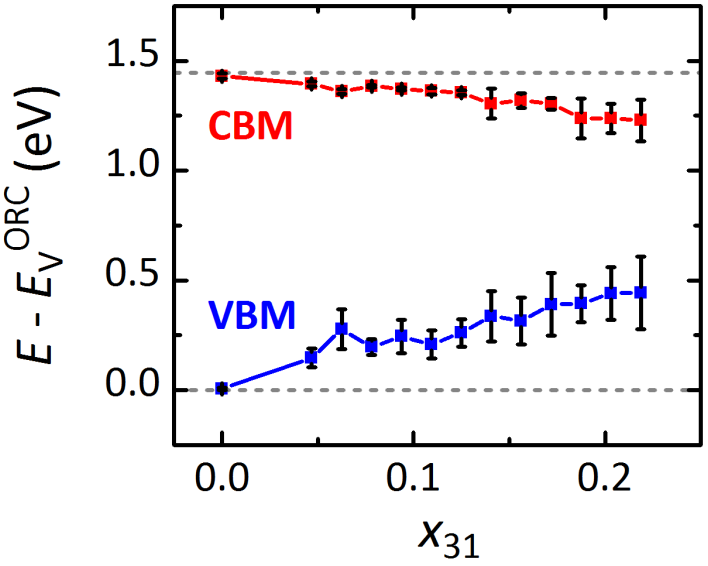

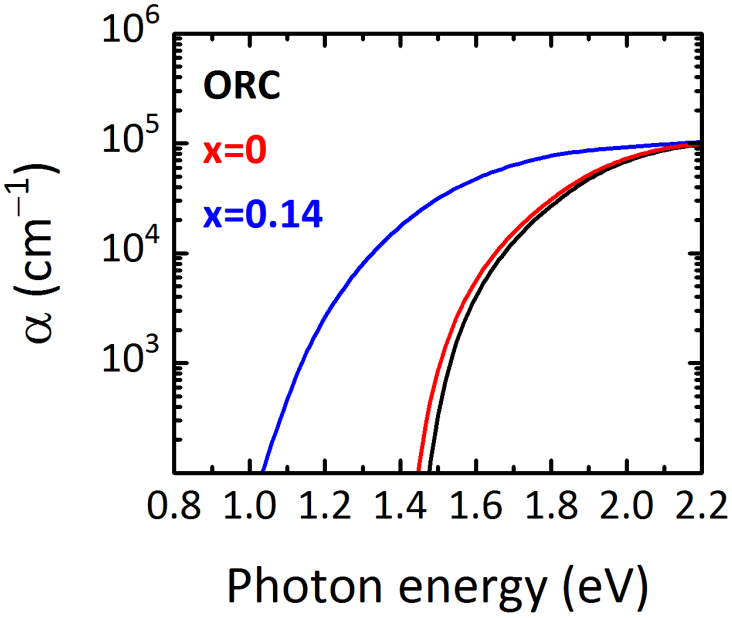

Band gaps and optical properties

- Valence conserving disorder (only Zn2Sn2 motifs) has virtually no effect, as compared to the perfectly ordered ORC structure
- Band gap shrinks with increasing x_{31}
- Absorption edge becomes less steep

Inverse Participation Ratio: Measure of localization

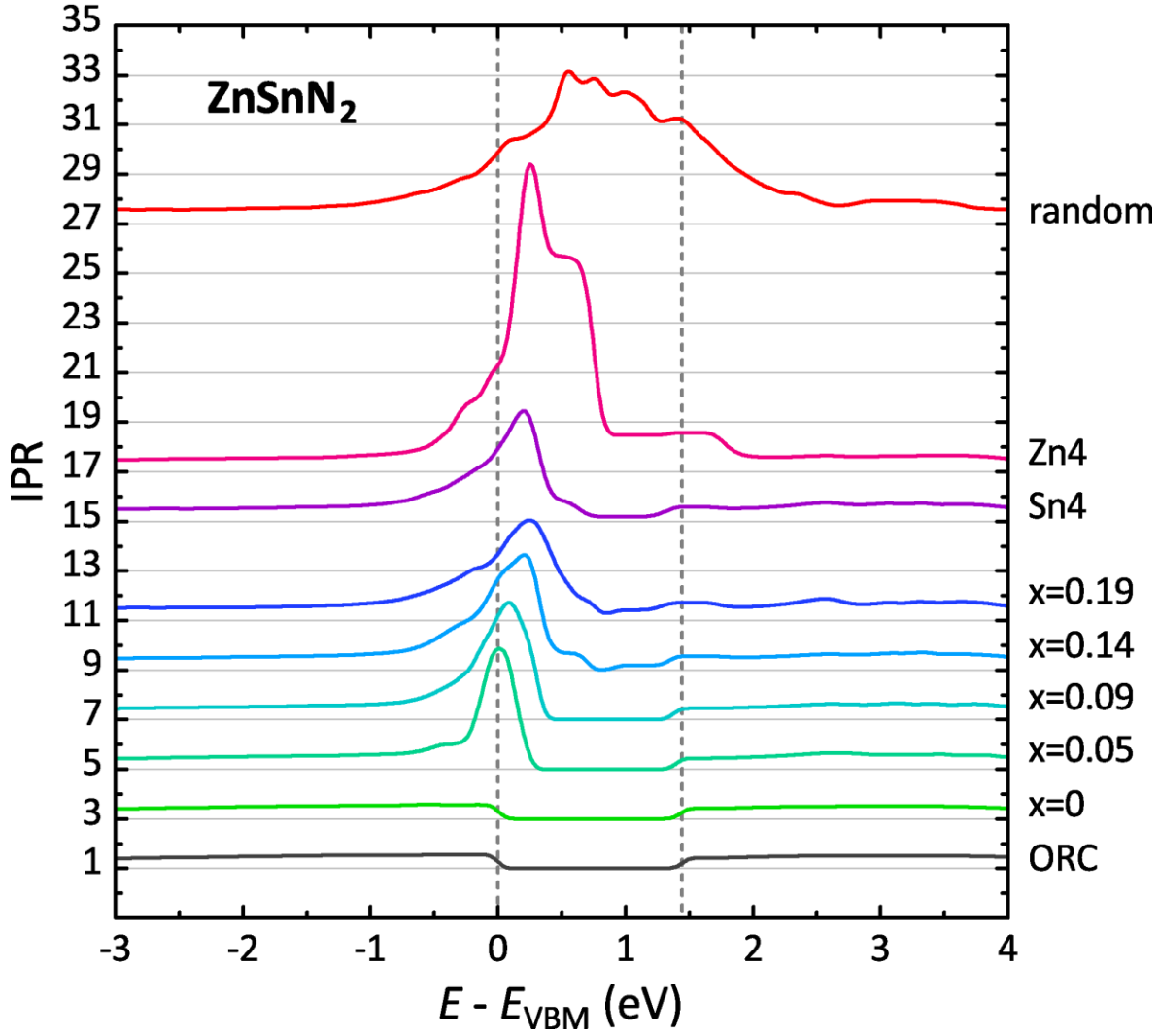

$$IPR(E) = \frac{N \sum_i p_i(E)^2}{\left(\sum_i p_i(E)\right)^2}$$

$p_i(E)$: atomic density of states

For example, IPR=10 means DOS is localized on 1 out of 10 atoms

- Octet-rule conserving disorder is benign
- "31" disorder causes only moderate localization
- Zn4 motifs create localized VB derived gap states
- Total random disorder fills gap with localized defect states

Conclusions

- **Electronic structure**
  Many-body perturbation theory in GW approximation Band-gaps, band-structure, optical properties
- **Defects**
  Defect formation energies, dopant-defect pair interaction
  Thermodynamic modeling, “defect phase diagrams”
- **Disorder**
  Model-Hamiltonian for total energy: Motif expansion
  Monte-Carlo simulations for atomic structure
  Electronic structure for disordered compounds
- **http://materials.nrel.gov**
  Database for DFT and GW calculations